

Innovative Development of a Soft Robotic Gripper: Mathematical Modelling and Grasping Capability Analysis

Hiep Xuan Trinh^a, Chu Anh My^{b*}, Phung Van Binh^c and Le Chi Hieu^d

^aFaculty of Mechanical Engineering, Le Quy Don Technical University, Hanoi, Vietnam;

^bInstitute of Simulation Technology, Le Quy Don Technical University, Hanoi, Vietnam;

^cFaculty of Aerospace Engineering, Le Quy Don Technical University, Hanoi, Vietnam;

^dFaculty of Engineering and Science, University of Greenwich, Kent ME4 4TB, United Kingdom

CONTACT: Chu Anh My. Institute of Simulation Technology Le Quy Don Technical University 236 Hoang Quoc Viet, Cau Giay, Hanoi 100000, Vietnam. Email: myca@lqdtu.edu.vn

Innovative Development of a Soft Robotic Gripper: Mathematical Modelling and Grasping Capability Analysis

Grasping or gripping is essential for both humans and robots. Soft and flexible grippers have been the focus of recent research due to their safe interaction with objects. However, most soft grippers rely on complex mechanisms or complicated structures, leading to challenging fabrication and modeling. Furthermore, there is a lack of mathematical models to estimate curvature shape, analyze gripping capacity, and stability under dynamic motion. To address these challenges, this study presents an innovative soft-fingered gripper design with an asymmetric tube that has a variable cross-section, providing a simple yet effective solution for gripping tasks. The proposed mathematical modeling and solutions were successfully developed and experimentally validated to analyze the effects of the robot arm's motion on the gripping capability of the gripper. Specifically, the mathematical modelling considers the effect of forces/moments imposing on the gripping mechanism of soft fingers, including the contact forces between the soft fingers and gripping objects. The proposed mathematical modeling and simulations can be used to analyze the deformation, gripping manipulations, and grasping capability of the soft-fingered grippers. This innovation represents an improvement over existing designs and has the potential to enhance the design and efficient performance of soft robotic grippers.

Keywords: Soft robotic gripper, mathematical modeling, robotic simulations, robotic dynamics.

1. Introduction

Grasping or gripping refers to the physical action of holding something; it is a common but very important function in both human and robotic manipulations. Humans can grip a wide range of objects with high precision, including rigid, soft, or delicate objects with various properties of size, shape, or texture, due to the natural softness attribute of the soft fingertips and multiple somatosensory receptors under the epidermis (Wen et al., 2020; Vedhagiri et al., 2019). In comparison with human gripping manipulation, robots have a relatively limited dexterous and adaptable grasping ability, because of a lack of

sophisticated sensing systems and negative effects of inherent properties of conventional robot hands such as rigid or complex kinematics, and control (Kleeberger et al., 2020; Bullock et al., 2013). Especially, the traditional rigid robot-fingered hands are generally difficult to implement grasping tasks with deformable or fragile objects without causing damages, due to the risk of exerting more excessive forces on the gripping objects than needed (Roa and Suárez 2015; Terrile, Argüelles, and Barrientos 2021). To guarantee stable and safe grasping manipulations, conventional robotic grippers require a sophisticated controller and tactile sensing system for monitoring the exact contact force (Hasan, Gerez, and Liarokapis 2020; Spiers et al. 2016). For purposes of improving the dexterous grasping ability of robotic hands, many anthropomorphic robotic gripper designs have been proposed, that attempt to mimic the human hand's gripping manipulations (Llop-Harillo et al. 2019; Watanabe et al. 2021). A few decades ago, soft robotic grippers have been introduced as a novel device that has exposed many benefits of dexterous gripping manipulation with delicate objects in unstructured environments. Generally, the soft-fingered hand is fabricated by soft materials such as silicone elastomers, urethane, hydrogels, and so on (Lee et al. 2017; Manti, Cacucciolo, and Cianchetti 2016). Exploiting the softness and deformable properties of the soft material, the soft robotic gripper is inherently compliant and able to maintain the contact area, resulting in large frictional force and moment without needing large contact forces, leading to safe interaction with the grasping objects.

Conceptually, the soft gripper can be characterized based on three main grasping mechanisms: actuation (Stuart et al. 2017; Yap, Ng, and Yeow 2016), controller stiffness (Hubbard et al. 2017), and controller adhesion (Shintake et al. 2016). Based on the actuation mechanism, the soft gripper can perform the grasping/gripping operation through the compliant deformation of the soft body using pneumatic (Guo et al. 2018) ,

or hydraulic actuators (Park et al. 2020), and tendon-driven (Ren et al. 2020), or shape memory alloy (Wang and Ahn 2017). For instance, Park et al. (Park et al. 2020) introduced the soft gripper based on the electrohydraulic actuator, fabricated by polyethylene film and silicone material. Galloway et.al., developed the soft robotic gripper based on soft pneumatic actuators, to delicately manipulate and sample fragile species on the deep reef (Galloway et al. 2016). V.Ho and S. Hirai proposed the soft-fingered hand with the contact feedback with the unbalanced deformation mechanism based on a novel concept of morphological computation (Ho and Hirai 2017). In such a design, the curvature gripping shape of the soft finger is generated from different elastic energy of multiple layers; nonetheless, the proposed soft hand requires the external motor to pull or release the tendon string for controlling the opened state of soft fingers.

The design of soft grippers with the mechanism of electroactive polymers or shape memory material has the advantage of enabling the flexibility of actuator configurations, that can be applied to develop different varieties of devices and robots; however, a high voltage is required for activations (typically several kV) (Marette et al. 2017), and a fabrication process is complicated (Carpi, Salaris, and De Rossi 2007; Rodrigue et al. 2017). Meanwhile, the gripping mechanism based on the variable stiffness materials generates the grasping force based on the variation of local stiffening of the structure. The gripper structure approaches and envelops the grasped object in the soft state of material; then the material is translated to be hard under external activations of vacuum (Loeve et al. 2010), heat (Al-Rubaiai et al. 2019), or electric field (Bhattacharya, Beperi, and Bhaumik 2014), resulting in a high holding force with minima object' compression. Many variable stiffness materials were used such as granular jamming, low-melting-point alloys, electrorheological and magnetorheological fluids, and shape-memory materials.

Basically, the gripping methods based on electroactive polymers or shape memory materials, variable stiffness materials, soft pneumatic and electrohydraulic actuators, can be applied to grasp objects with various shapes and sizes; however, it is required to use the external devices such as pumps, vacuum chambers, or heating elements, leading to the complicated fabrication and high costs.

In terms of the controlled adhesion mechanism, the soft gripper uses the interface attraction between two surfaces to generate the holding force (Hu, Dong, and Sun 2021; Shintake et al. 2016) . This mechanism improves the dexterity and versatility of soft grippers but it also requires advanced technologies to generate a compliant surface with high attractive force.

It has been well-documented that, pneumatic and hydraulic actuating mechanics have recently been widely utilized in the design of soft grippers, due to their advantages such as low cost, high gripping efficiency, simple fabrication, easy control, and fast responses. As a result, most soft-fingered grippers are currently designed based on pneumatic or hydraulic actuation, often consisting of serial chambers with specially designed thin walls to generate the gripping shape under pressurization activation. However, the design of thin walls in these grippers can lead to failures such as tearing, wearing, or bulging. Furthermore, the construction with thin wall chambers makes fabrication difficult and creates complications in mathematical models used to estimate curvature shape or contact gripping forces. Alternative designs of soft grippers have been proposed, such as the mechanism of an asymmetric tube actuator. In another publication (Mata Amritanandamayi Devi, Udupa, and Sreedharan 2018), the under actuated multi fingered soft robotic hand was introduced for prosthetic applications, which combined thin wall chambers and an asymmetric tube with a constant cross-section to assist gripping tasks. While effective, this design was still complex, and the

deformation of the soft finger under hydraulic/pneumatic actuation was curved with a constant radius, which is not optimal for gripping. The curvature of the soft finger is expected to be larger at the tip and smaller at the base. This has led to the suggestion that the soft gripper's finger should feature a variable cross-section to achieve a more appropriate deformation for gripping purposes. More importantly, the approaches mentioned above did not include explicit mathematical equations for the curvature of the soft finger and only focused on the robustness of gripping manipulation. Consequently, there is a lack of mathematical models to estimate the curvature shape, analyze the gripping capacity, and assess the stability of these soft-fingered grippers during dynamic motion. Soft grippers are usually mounted on robot arms during gripping manipulations, making the gripping process complex and influenced by various parameters, such as weight, the shape of the objects being gripped, and inertia due to the acceleration of the robot arm. Therefore, it is imperative to develop a novel theoretical approach to study the gripping capability of the soft gripper under dynamic motion, especially in the context of the growing use of collaborative robots in Smart Manufacturing and Industry 4.0 (Le et al. 2020).

Similar to human grasping, the stability of a grasped object depends on the local curvature properties at the contacts, as well as the magnitude and arrangement of the applied forces (Burstedt, Flanagan, and Johansson 1999; Howard and Kumar 1996). For conventional gripper, with the innovative design of joints and links, the grasping shapes and forces of conventional grippers can be mathematically described, thus its grasping can be evaluated by explicit models. For instance, D. Wang et.al., presented the kinematics and statics analysis of the grasping performance of a passively adaptive five-fingered under actuated dexterous hand based on the principle of virtual work. The model of the contact force of each phalanx was then solved by several numerical calculations to

clarify the effect of the contact position and bending angle on the contact force (Wang et al. 2021). Mathematical models based on constraint analysis are also used to calculate the forces in joints, then evaluated the grasping capability of the gripper (Liu et al. 2021). In (ACAR, SAĞLAM, and ŞAKA 2021), the grasping capacity of the conventional gripper with a spherical and a planar mechanism was evaluated, using the analysis of equilibrium equation systems of objects and fingers.

Compared to conventional grippers, the soft gripper relies on the deformation of soft materials to generate the grasping form, making it challenging to mathematically describe its gripping manipulation capability due to the physical and geometrical nonlinearities associated with the large deformation of soft materials. Existing research on soft grippers has primarily focused on kinematic and static modelling. Different approaches have been proposed, such as the Cosserat theory (Haibin et al. 2018), Euler-Bernoulli beam-based constant and variable curvature method (Webster and Jones 2010; Zhong, Hou, and Dou 2019), screw theory (Hussain et al. 2021), or finite element models (Yarali et al. 2020). In (Haibin et al. 2018), the authors used the Cosserat theory to calculate the grasping force at the fingertip of the soft gripper with variable stiffness that was subjected to complex forces of gravity, grasping forces, and driving torques. The screw theory was applied to analyze the contact force for a compliant gripper with a structure composed of rigid links connected through compliant joints and soft pads (Hussain et al. 2021). Wang presented the linear segment model to estimate the curvature shape of the printed-soft finger and the contact forces at the fingertip (Wang and Hirai 2017). Nonetheless, most of the above-mentioned methods proposed the analytical model to consider the curvature shape of the soft finger in its free state, which did not account for the external loads, and the contact forces normally were calculated at the position of

the fingertip. When investigating the capability of the soft gripper with multiple fingers, the contacts at several points on grasping objects need to be considered.

To address the above issues, this paper proposes an innovative design for a soft-fingered gripper with a curvature shape mechanism, based on the working principle of the soft pneumatic actuator. This design is simpler than the popular serial thin wall chamber design, making fabrication and modelling easier and avoiding common issues such as torn, worn, and bulging. The variable cross-section of the design allows for more suitable deformation of the fingers when gripping objects. Each soft finger includes a strain-gauge sensor to generate a contact feedback signal, used to analyze the gripping object's stability during the grasping process. To evaluate the grasping capability of the proposed gripper, a novel theoretical approach is proposed, bridging the deformation and gripping models of the soft finger. The effect of the dynamic motion on the soft gripper's capability is considered. The curvature deformation of the soft finger is modeled by an explicit mathematical equation based on the theory of a large deformation beam. This model is used to build an equivalent model of discrete serial rigid links with rotational joints and torsional moments, allowing for continuous linkage from the deformation model to the dynamics model of the finger. The contact forces at multiple contact points during grasping manipulation are described by explicit mathematical equations, taking into account the motion's acceleration of the robot arm. A solution based on the numerical method is developed to investigate the effect of the robot arm's motion on the grasping capability of the soft gripper. Finally, the effectiveness of the proposed methods is validated through experiments.

2. Development of a Soft-fingered gripper

2.1. Mechanism of Soft Fingers

The proposed robotic gripper has soft fingers to implement the grasping manipulation, in which, the curvature shape of the soft fingers is generated based on the deformation of the soft actuator, which is an asymmetric tube with a variable cross-section. Figure 1 presents the working mechanism of a soft finger, in which the bending curvature of the soft finger is based on the deformation principle of an asymmetric soft actuator. The detail of a 3D model and dimensions of a soft finger of a proposed soft-fingered gripper is shown in Figure 2; the soft finger has a similar size of the human finger. The asymmetric tube is innovatively designed as a circular cross-section with different thicknesses of the top and the bottom side. Due to the different thicknesses and stiffness between two sides of the asymmetric tube, under the actuation of the internal pressure, the actuator is bent in the direction of the thicker side. To mimic the gripping shape of the human finger, the curvature deformation must be well-controlled, the thickness of two sides of the soft fingers, therefore, needs to be variable along their length. To improve the gripping contact area, the thicker side of the soft finger is designed to be partly flat. At the free-end, the soft finger is chamfered, with the embedded rigid nail to limit the tip inflation and make better pick-and-place performance of the soft finger. The air pressure enters the soft finger from the fixed end through a small tube. The bending curvature of the soft finger depends on its geometrical designs and pressure values.

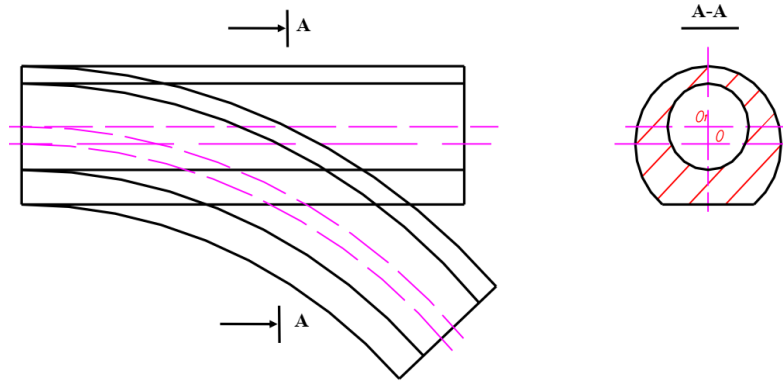


Figure 1. The bending curvature of the soft finger based on the deformation principle of the asymmetric soft actuator.

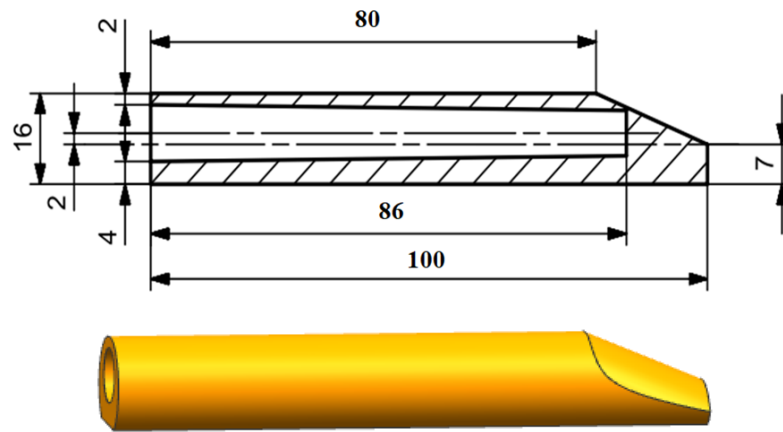


Figure 2. 3D model and dimensions of a soft finger of a proposed soft-fingered gripper.

2.2. Design of a soft-fingered gripper

The soft fingers are assembled into a gripper that can attach to the robot's arm. The gripper includes three soft fingers, three rigid connectors, and a rigid box. Three rigid connectors are used to clamp the fingers and attach to the rigid box by threaded joints. The rigid box is fixed to the robot arm by screws. The strain gauges are embedded in the soft fingers to detect the contact manner between the gripper and grasping objects. The whole gripper with soft fingers is depicted in Figure 3.

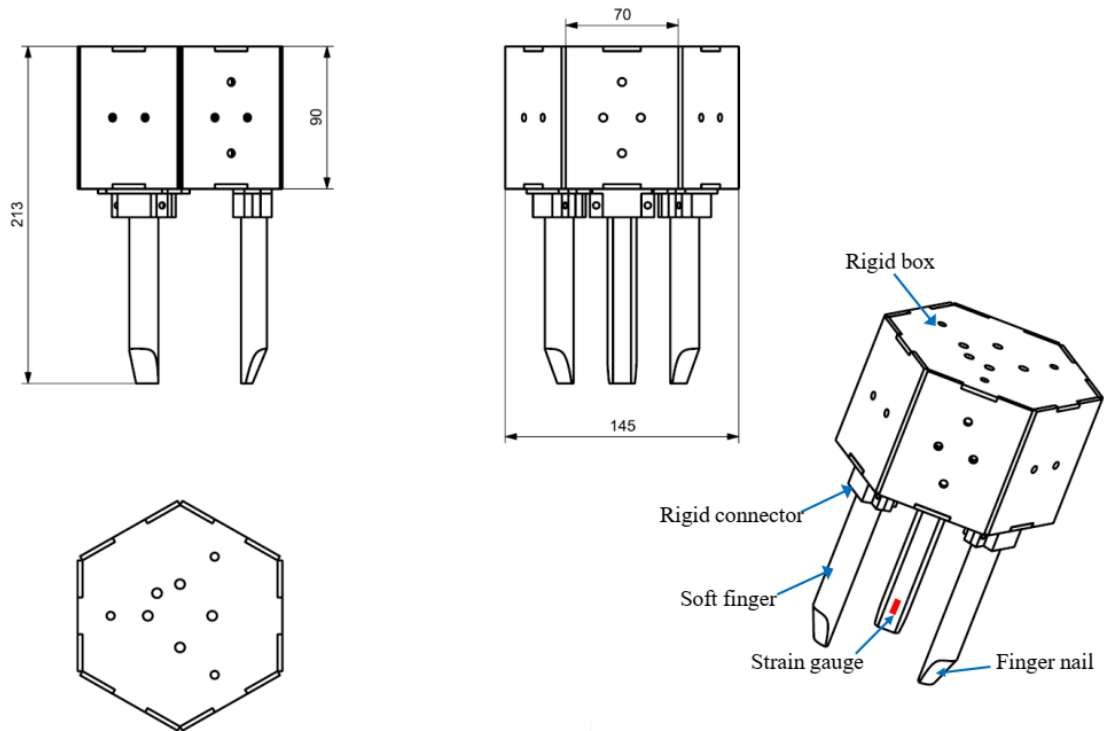


Figure 3. Design of soft fingered-gripper.

2.3. Fabrication of a soft-fingered gripper

The soft fingers were made from the silicone rubber of RTV 225, and it was fabricated with the use of two 3D-printed molds. Figure 4 and Figure 5 present the design of a fabrication mold and the description of a fabrication process of soft figures based on the molding method.

Two molds are used to fabricate a soft figure as shown in Figure 4. The first mold has three parts and it is used to fabricate the main part of the soft finger, and the second mold is used to seal the fixed end of the finger. The fabrication process of the soft finger by the molding method can be summarized as follows (Figure 5). Firstly, two components of the liquid silicone rubber are mixed with a ratio of 1:1, then the mixed liquid silicone is poured into the assembly mold, and it is cured at room temperature for ten hours. After the curing process is fully completed, the lower and upper cavities of the mold are removed to get the main part of the soft finger. At this stage, the soft finger still has an

open end, which is then closed with the same mixed silicone, via the use of the second mold, with a similar curing process, and finally, the soft finger is fully fabricated. The strain gauges are then embedded into the soft fingers with special glue. The rigid connectors and rigid box were designed with the use of the common CAD software, Solidworks (Dassault Syst`emes), and they were fabricated by CNC with laze cutting machine C02 HK-LS6090 and Additive Manufacturing with 3D printer Zortrax M300. The fabricated soft fingers are finally assembled and fixed to the connector and the rigid box, to fully make the soft-fingered hand.

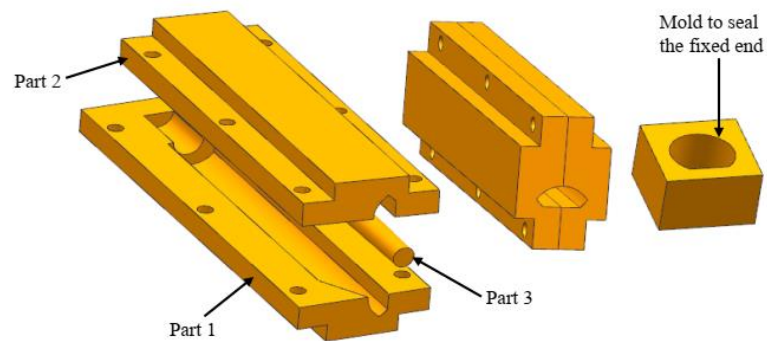


Figure 4 . 3D models of a mold that is used to fabricate soft fingers.

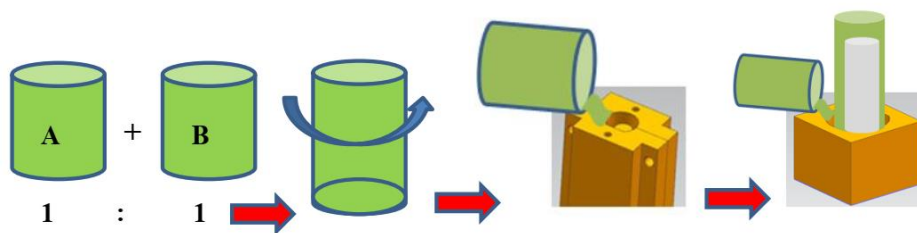


Figure 5. A fabrication process of soft fingers based on the molding method

3. Deformation modelling of a soft finger

3.1. Finite element model of soft finger's deformation

To evaluate the effectiveness of gripper design and better understand the deformation of the soft finger, firstly, the numerical simulation was done by using the commercial software Abaqus (ABAQUS Inc.). In which the standard model with an explicit algorithm

was used. The soft actuator was modeled as a deformable solid with the hyper-elastic material model. The Yeoh model with the parameters of $C_{10} = 0.1$, $C_{20} = 0.02$, $C_{30} = 0.0002$, $D_1 = D_2 = D_3 = 0$ (Dang et al. 2021), was used in the simulations. The developed Finite Element Analysis (FEA) model uses the linear hexahedral elements of type C3D8R with a global mesh seed of $1.5mm$. The deformation of the soft finger was simulated by using static analysis, where the gripper is bound to fix one end, and the other end is free. The effect of air pressure actuation was modeled by uniformly distributed pressure on the internal surfaces of the soft finger's cavity. The setting of the analysis step includes the nonlinear effects of large displacements. The range of pressure values was varied from $60kPa$ to $160kPa$ to investigate its values' effect on the curvatures of the soft finger. The simulated deformation of the soft finger is shown in Figure 6. From the finite element simulation results, it can see that under the pressure's activation with the value range of $60kPa$ to $160kPa$, the curvature deformation of the soft finger is small with values of $60kPa$ and $80kPa$. Still, it increases significantly under the range of $100kPa$ to $160kPa$. Thus, the gripper design with the soft finger can effectively manipulate the gripping tasks, and the suitable values of the pressurization activation are from $100kPa$ to $160kPa$.

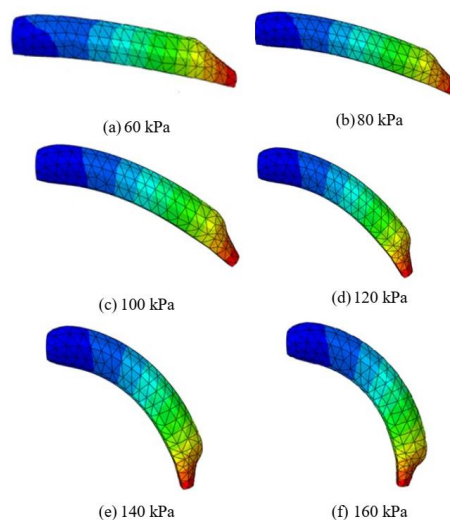


Figure 6. Simulation of soft finger's deformation

3.2. Mathematical formulation of a soft finger's curvature

In order to model the deformation of a soft figure, it is necessary to develop mathematical models to estimate the curvature deformation of the soft finger under the activation of the pressurization. Figure 7 presents a schematic of large deformations of a cantilever beam with a variable cross-section. It is assumed that the soft finger's deformation is modeled as the cantilever beam in which one end is fixed, and the other end is free, subject to a concentrated moment. To simplify the calculation, the mechanical properties of soft material are assumed as linear; the Young modulus $E = 550Pa$ is used (Dang et al. 2021).

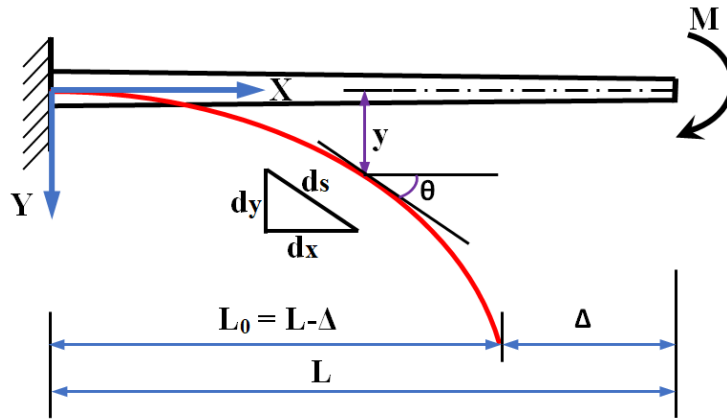


Figure 7. A schematic of large deformations of a cantilever beam with a variable cross-section

Based on the Euler–Bernoulli law, in Cartesian coordinate, as described in Figure 7, the large bending deformation of the cantilever beam with a variable cross-section is expressed as:

$$\frac{(1 + y'^2)^{\frac{3}{2}}}{y''} = -\frac{EI_x}{M} \quad (1)$$

where y is the vertical deflection of the cantilever beam at any horizontal position, y' and y'' is the first and second derivative of vertical deflection y with respect to variable x , E is the Young modulus of the material, M is the concentrated bending moment at the free

end, caused by the activation effect of the air pressure and I_x is the inertia moment of variable cross-section. I_x is dependent on the position of the cross-section, and it is a function of the variable x . The determination of I_x is expressed in the appendix.

The concentrated moment M is defined as follows:

$$M = eF^* \quad (2)$$

where e is the eccentric of the soft finger's cross-section and F^* is the equivalent activated force of air pressure. The value of e and F^* are calculated as the following:

$$e = \frac{e_1 + e_2}{2} \quad (3)$$

$$F^* = p\pi \left(\frac{d_1 + d_2}{2} \right)^2 \quad (4)$$

where (e_1, e_2) , (d_1, d_2) is the maximum, and minimum values of the eccentric, and tube's diameter at two end cross-sections of the soft finger, respectively.

By setting $y' = \rho$, $\lambda_x = -\frac{M}{EI_x}$, equation (1) can be rewritten as:

$$\frac{d\rho}{(1+\rho^2)^{\frac{3}{2}}} = \lambda_x dx \quad (5)$$

To solve the above equation, we set $\rho = \tan \theta$, then we have:

$$d\rho = \frac{1}{(\cos \theta)^2} \quad (6)$$

$$(1+\rho^2)^{\frac{3}{2}} = \left(\frac{1}{(\cos \theta)^2} \right)^{\frac{3}{2}} \quad (7)$$

From equations (6, 7), equation (5) can be rewritten as follow:

$$\int \cos \theta d\theta = \int \lambda_x dx \quad (8)$$

Then, we have:

$$\sin \theta = \varphi(x) + C \quad (9)$$

where $\varphi(x) = \int \lambda_x dx$ and C is a constant.

Note that:

$$\sin \theta = \frac{\sin \theta / \cos \theta}{1 / \cos \theta} = \frac{\tan \theta}{\sqrt{1 + (\tan \theta)^2}} = \frac{\rho}{\sqrt{1 + \rho^2}} \quad (10)$$

From equations (9, 10), we have the following equations:

$$\begin{aligned} \frac{\rho}{\sqrt{1 + \rho^2}} &= \varphi(x) + C \\ \frac{\rho^2}{(1 + \rho^2)} &= (\varphi(x) + C)^2 \\ 1 - \frac{1}{1 + \rho^2} &= (\varphi(x) + C)^2 \\ 1 + \rho^2 &= \frac{1}{1 - (\varphi(x) + C)^2} \\ \rho &= \frac{\varphi(x) + C}{\sqrt{1 - (\varphi(x) + C)^2}} \end{aligned} \quad (11)$$

By setting $G(x) = \varphi(x) + C$ and replacing $\rho = y'$. Finally, we have:

$$y' = \frac{G(x)}{\sqrt{1 - (G(x))^2}} \quad (12)$$

Where C is the constant of integration which can be determined from the boundary conditions $y' = 0$ at $x = L_0 = L - \Delta$ (Figure 7). By applying this condition to equation (12), we get: $C = -\varphi(x)|_{x=L-\Delta}$

Note that $G(x)$ in equation (12) is a function of the unknown horizontal displacement Δ of the free end of the beam. The value of Δ can be determined based on the assumption of the beam's length is constant. The differential length of the beam ds can be calculated as the following mathematical transformation (Figure 7).

$$ds = (dx^2 + dy^2)^{1/2} = \frac{(dx^2 + dy^2)^{1/2}}{dx} dx = (1 + (y')^2)^{1/2} dx \quad (13)$$

From equation (13), the beam's length L can be calculated as follow:

$$L = \int_0^{L_0} (1 + (y')^2)^{1/2} dx \quad (14)$$

Replacing equation (12) into equation (14), we have:

$$L = \int_0^{L_0} \frac{1}{\sqrt{1 - (G(x))^2}} dx \quad (15)$$

where $L_0 = L - \Delta$

Note that: $G(x)$ and L_0 are functions of the unknown parameter Δ . From equation (15), the value of Δ can be calculated by using a trial-and-error procedure (Anon 2006). The trial-and-error procedure is started with a specific value of Δ , then it may be repeated for various values of Δ until the obtained length from equation (15) is correct to the actual length with a small error. This procedure is implemented in MATLAB (The MathWorks, Inc.), in which the error is set between the calculated beam's length and its actual value is 5% to stop the repeated process.

After determining the value of Δ , the function $G(x)$ only depends on the variable x . And the vertical deflection of the cantilever beam at any horizontal position is calculated as:

$$y = \int_0^x \frac{G(x)}{\sqrt{1 - (G(x))^2}} dx \quad (16)$$

By calculating the vertical deflection y at various horizontal positions x , we can estimate the bending curvature of the soft finger under pressurizations, using the integration function in MATLAB¹.

¹ <https://www.mathworks.com/help/matlab/ref/integral.html> (assessed on 6/27/2022)

4. Dynamic performance and gripping capability analysis of soft fingers

4.1. Mathematical modelling of a gripping mechanism

To investigate the performance and gripping capability of the soft finger, the dynamic modelling of the gripping mechanism is proposed in this study, with a focus on describing the contact forces at multiple contact points between the soft fingers and gripping objects. Under the impact of air pressurization actuation, the soft finger is deformed with a curvature shape and is described by the explicit mathematical equation (16) in Section 3.2. To develop the mathematical model of contact forces, based on the idea of the pseudo-rigid-body model approach for compliant mechanism (Chase et al. 2011; Chu et al. 2022; My and Bien 2020; Wang and Chen 2009), the soft finger is modeled into n rigid links with the corresponding n consecutive lines, as shown in Figure 8(a). The schematic equivalent rigid links model of the soft finger is described in Figure 8(b).

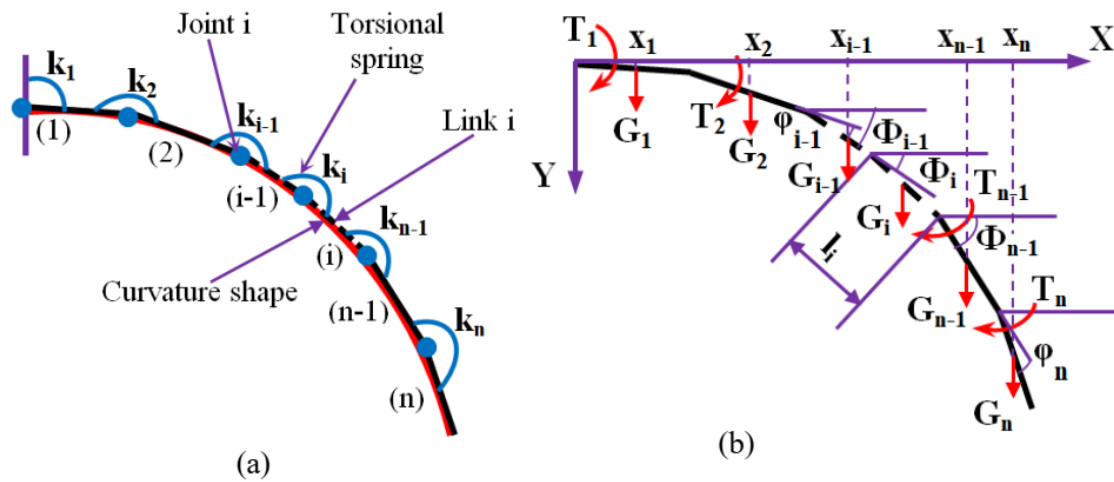


Figure 8. Modeling soft finger by serial rigid links with rotational joints and torsional springs

The equivalent model is proposed based on assumptions: (i) The i^{th} line is the tangent of the curvature at the midpoint positions with horizontal coordinate x_i . (ii) The i^{th} links have the constant length l_i and its weight is converted to the concentrated weight $G_i = gm_i$ at the midpoint. (iii) The connections between two consecutive links are

represented as the rotational joint and torsional spring with the stiffness of k_i . (iii) The activation of the air pressure is modeled as a series of torsional moments T_i , which is located at the corresponding joint i^{th} (As described in Figure 8(b)). Under the activation of the moment T_i , the i^{th} link rotates at a relative angle φ_i with the $(i - 1)^{th}$ link and Φ_i with the horizontal axis OX (Figure 8(b)). The values of the horizontal coordinate x_i depend on the curvature shape of the beam and the divided number of the equivalent links. The values of x_i can be estimated as follows. The soft gripper is modeled into n rigid links; each link is a line $A_{i-1}A_i$ and has a predetermined constant length l_i . With the last link (n^{th} link), the horizontal coordinate of the point A_n is determined as:

$$x_{A_n} = L - \Delta \quad (17)$$

Where Δ is calculated as in Section 3.2. The value of the vertical coordinate y_{A_n} of point A_n is determined through the equation of the curvature shape (equation (16) in Section 3.2). Thus, the coordinate of point A_n is determined. Then the coordinate of point A_{n-1} is estimated as an intersection of a circle with center point A_n , radius l_n , and the curvature's soft finger (Figure 9). After that, the value of x_n is estimated as:

$$x_n = \frac{x_{A_{n-1}} + x_{A_n}}{2} \quad (18)$$

Similarly, we can estimate the value of $x_{n-1}, \dots, x_i, \dots, x_1$.

After estimating the values of horizontal coordinate x_i , the configuration parameters of the equivalent model are determined as the follows: Due to the assumption of the i^{th} link is the tangent of the curvature at the position x_i , we can estimate the value of the angle Φ_i as the follows:

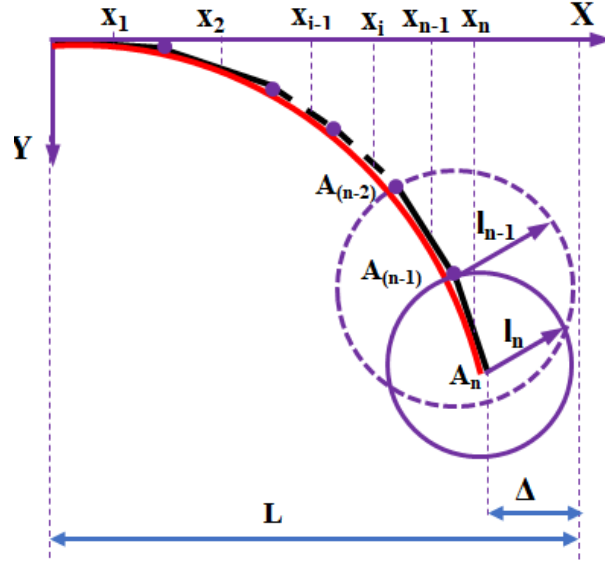


Figure 9. Modeling soft finger by serial rigid links with rotational joints and torsional springs

Due to the assumption of the i^{th} link is the tangent of the curvature at the position x_i , we can estimate the value of the angle Φ_i as the follows:

$$\tan \Phi_i = y'_{(x_i)} \quad (19)$$

Then, we have:

$$\Phi_i = \arctan\left(y'_{(x_i)}\right) \quad (20)$$

In terms of the relative angle φ_i as seen in Figure 8(b), the following relationship is obtained:

$$\begin{aligned} \Phi_1 &= \arctan\left(y'_{(x_1)}\right) \\ \Phi_2 &= \Phi_1 + \varphi_2 = \arctan\left(y'_{(x_2)}\right) \\ &\dots \\ \Phi_i &= \Phi_{i-1} + \varphi_i = \arctan\left(y'_{(x_i)}\right) \\ \Phi_n &= \Phi_{n-1} + \varphi_n = \arctan\left(y'_{(x_n)}\right) \end{aligned} \quad (21)$$

Generally, the relationship between the angle φ_i , and Φ_i can be expressed as follows:

$$\Phi_i = \sum_{j=1}^{j=i} \varphi_j = \sum_{j=1}^{j=i} \arctan\left(y'_{(x_j)}\right) \quad (22)$$

Thus, we can calculate the angle φ_i as below:

$$\varphi_i = \arctan\left(y'_{(x_i)}\right) + \sum_{j=i-1}^1 (-1)^{i-j} \arctan\left(y'_{(x_j)}\right) \quad (23)$$

Then, the stiffness of the torsional spring is calculated as below:

$$k_i = \frac{T_i}{\varphi_i} \quad (24)$$

Based on equation (24), the virtual loading method to determine the stiffness value k_i of the i^{th} torsional spring can be developed. Figure 10 presents a schematic model of the virtual loading to determine the torsional stiffness.

The following is the detailed description of the proposed virtual loading method, which is used to determine the stiffness value k_i of the i^{th} torsional spring. First of all, it is supposed that the soft finger has a fixed end and the other end is subjected to a concentrated force F . Under the activation of the concentrated force F , the soft finger is deformed, and its curvature shape can be mathematically described by equation (16), in which the moment M is replaced by a moment M_F , that is calculated as:

$$M_F = Fl \quad (25)$$

After estimating the curvature of a soft finger, from equations (22), and (23), we can estimate the deviation angle φ_i^F between two consecutive the $(i-1)^{th}$ link with the i^{th} link and the angle Φ_i^F between the i^{th} link with the horizontal axis OX.

$$\Phi_i^F = \sum_{j=1}^{j=i} \varphi_j^F = \sum_{j=1}^{j=i} \arctan\left(y'_{F(x_j)}\right) \quad (26)$$

$$\varphi_i^F = \arctan\left(y'_{F(x_i)}\right) + \sum_{j=i-1}^{j=1} (-1)^{i-j} \arctan\left(y'_{F(x_j)}\right) \quad (27)$$

where y_F and $y'_{F(x_i)}$ is the mathematical equation of curvature shape in the case of concentrated force F and its derivative at the horizontal coordinate x_i , respectively.

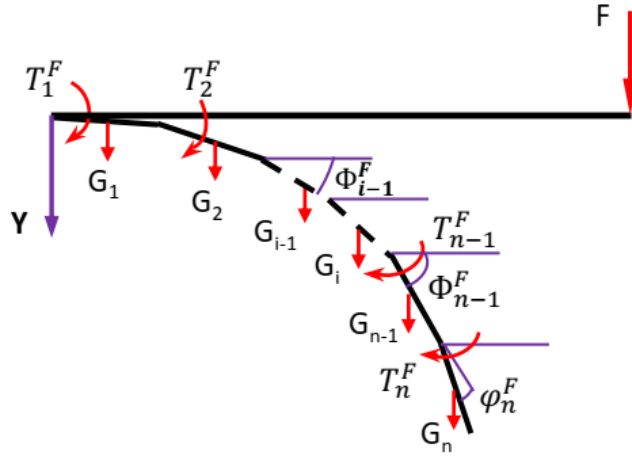


Figure 10. Schematic model of virtual loading to determine the torsional stiffness

The moment T_i at the i^{th} joint is calculated as:

$$T_i^F = k_i \varphi_i^F = F \left(\sum_{j=i}^n l_j \cos(\Phi_j^F) \right) + \frac{\sum_{j=i}^n m_j g l_j \cos(\Phi_j^F)}{2} + \sum_{j=i}^{n-1} m_{j+1} g l_j \cos(\Phi_j^F) \quad (28)$$

Then, from equation (24), the stiffness of the torsional spring is calculated as:

$$k_i = \frac{F \left(\sum_{j=i}^n l_j \cos(\Phi_j^F) \right) + \frac{\sum_{j=i}^n m_j g l_j \cos(\Phi_j^F)}{2} + \sum_{j=i}^{n-1} m_{j+1} g l_j \cos(\Phi_j^F)}{\arctan(y'_{F(x_i)}) + \sum_{j=i-1}^{j=1} (-1)^{i-j} \arctan(y'_{F(x_j)})} \quad (29)$$

After determining the stiffness k_i of the torsional spring, the configuration of the rigid equivalent links will be used in the model to describe the forces in the contact between the soft finger and the object during the grasping manipulation. Figure 11 presents a schematic model of forces and moments acted on the soft fingers.

In the equivalent rigid links, the contact zone is assumed within the boundary between i^{th} link and n^{th} link, thus the normal contact force F_n is only exerted on these links (Figure 11b), F_i^n is the normal force of the i^{th} link, and it is determined from the equilibrium of the soft fingers.

The equilibrium of the soft fingers can be expressed as the conservation of the total moment of the joints. That means the moment of the joints at the free state and the gripping manipulation state must be equal.

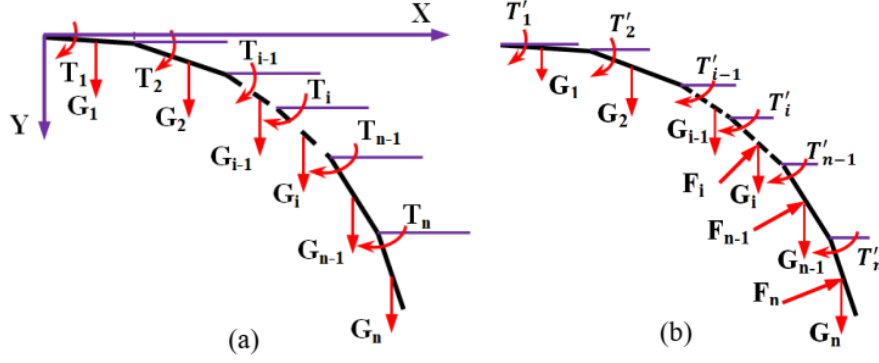


Figure 11. A schematic model of forces and moments acted on the soft finger at the free state (a) and the manipulation state (b).

The forces and moments of the last link (n^{th} link) are described in Figure 12(a) and its equilibrium equations can be expressed as:

$$\begin{aligned}
 F_n^x &= F_n^n \sin \Phi'_n \\
 F_n^y &= -F_n^n \cos \Phi'_n + G_n = -F_n^n \cos \Phi'_n + m_n g \\
 T_n &= k_n \varphi_n = T'_n - \frac{F_n^n l_n}{2} + \frac{m_n g l_n \cos \Phi'_n}{2} = k_n \varphi'_n - \frac{F_n^n l_n}{2} + \frac{m_n g l_n \cos \Phi'_n}{2}
 \end{aligned} \tag{30}$$

Then

$$F_n^n = \frac{2k_n \Delta \varphi_n + m_n g \cos \Phi'_n}{l_n} \tag{31}$$

where: $T'_n = k_n \varphi'_n$, $\Delta \varphi_n = \varphi_n - \varphi'_n$. Similarly, the forces and moments of the $(n-1)^{th}$ link are depicted in Figure 12(b) and its equilibrium equations can be expressed as:

$$\begin{aligned}
 F_{n-1}^x &= F_n^x + F_{n-1}^n \sin \Phi'_{n-1} \\
 F_{n-1}^y &= F_n^y - F_{n-1}^n \cos \Phi'_{n-1} + m_{n-1} g \\
 T_{n-1} &= k_{n-1} \varphi_{n-1} = T'_{n-1} - T'_n - \frac{F_{n-1}^n l_{n-1}}{2} - F_n^x l_{n-1} \sin \Phi'_{n-1} + F_n^y l_{n-1} \cos \Phi'_{n-1} \\
 &\quad + \frac{m_{n-1} g l_{n-1} \cos \Phi'_{n-1}}{2}
 \end{aligned} \tag{32}$$

Then,

$$F_{n-1}^n = \frac{2(k_{n-1}\Delta\varphi'_{n-1} - T'_n - F_n^n l_{n-1} \cos(\Phi'_n - \Phi'_{n-1})) + (2m_n + m_{n-1})gl_{n-1} \cos\Phi'_{n-1}}{l_{n-1}} \quad (33)$$

Generally, the normal force F_i^n (Figure 12(c)) can be calculated as:

$$F_i^n = \frac{2\left(k_i\Delta\varphi'_i - T'_{i+1} - F_{i+1}^n l_i \cos(\Phi'_{i+1} - \Phi'_i) - l_i \left(F_n^x \sin\Phi'_i - F_n^y \cos\Phi'_i\right)\right) + (2m_{i+1} + m_i)gl_i \cos\Phi'_i}{l_i} \quad (34)$$

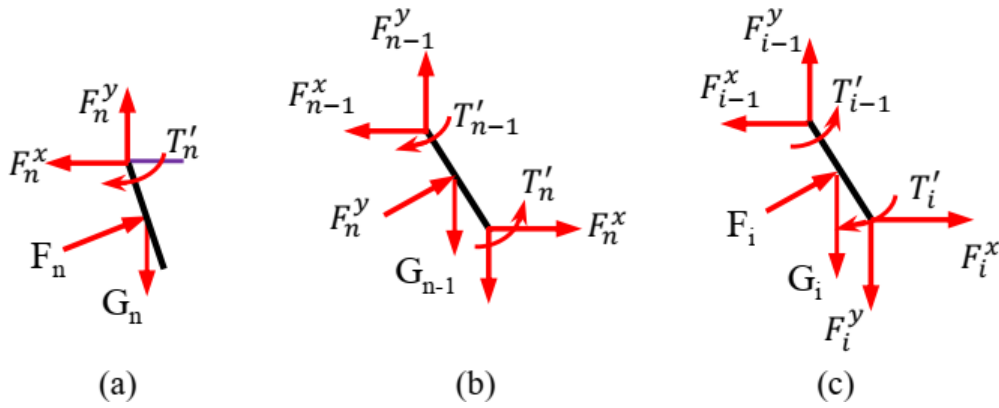


Figure 12 . Analysis of acted forces and moments of each link at the manipulation state.

(a) n^{th} link; (b) $(n - 1)^{th}$ link; (c) i^{th} link

Note that in equations (30) to (34), φ_i, φ'_i is the deviation angle between two consecutive links of the free and the gripping manipulation state. Φ'_i is the angle between the i^{th} link with the horizontal axis OX in the gripping manipulation state. The value of the angle φ_i is determined from equation (23), and the angle φ'_i , and Φ'_i is dependent on the contact object's profile and the contact position between the soft finger and the grasping object.

In this study, the gripping performance of the proposed soft-fingered gripper was investigated with the most popular gripping task of pick-and-placing manipulation, which has three-step as depicted in Figure 13. In the first step, the soft gripper makes contact with stationary objects and then picks them up in the vertical direction. In the

second step, the soft gripper moves horizontally to transfer the object from the picking position to the placed position. And finally, the soft gripper performs the placing manipulation. The grasping capability of the soft gripper can be assessed by the object's stability. It depends on the balance of the forces acting on the object.

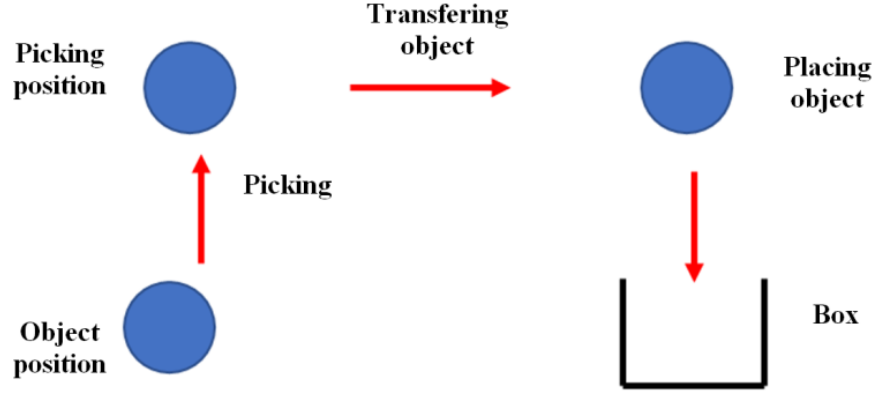


Figure 13. A schematic model of pick-and-placing manipulation of the soft gripper

The acting forces on the object include the frictional forces between the object and the soft finger, the gravitational force of the object, the normal forces, and the inertial forces, caused by the acceleration motion of the robot arm. Where the inertial forces is assumed as the concentrated forces at the gravity's center of the object (as depicted in Figure 14). The total generated frictional force in the contact zone F_T is changed, depending on the contact state stick or slip. For the stick case, friction force F_T increases, and $F_T < \mu F_N$, and in the slipcase $F_T = \mu F_N$, with μ is the frictional, coefficient. Hereafter, we estimate friction force F_T in the stick phase. The gripper's design uses three soft fingers with asymmetry positions. Thus, the equilibrium equations of the object are described as the following equation.

$$\begin{aligned} 3 \left(\sum_i F_i^n \cos \Phi'_i + F_i^T \sin \Phi'_i \right) &= mg + ma_y \\ 3 \left(\sum_i F_i^n \sin \Phi'_i + F_i^T \cos \Phi'_i \right) &= ma_x \end{aligned} \quad (35)$$

Where a_x and a_y are the acceleration of horizontal and vertical motion, respectively, and m is the mass of the object. The total generated frictional force in the contact zone F_T is:

$$F_i^T = 3 \sum_i F_i^T \quad (36)$$

Finally, the stability condition of the object in the grasping manipulation is written as follows:

$$\sum_i F_i^T < \mu \sum_i F_i^n \quad (37)$$

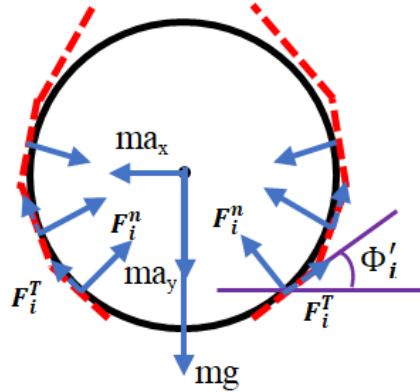


Figure 14. A schematic contact forces of object in the grasping manipulation

4.2. Simulations and evaluations of the theoretical model of gripping mechanism

In the theoretical model of contact forces, the angle ϕ_i' , and Φ_i' are the random parameters. These values depend on the shape of contact objects, and contact positions, which cannot be predetermined before implementing the grasping tasks. Thus, to validate the effectiveness of the theoretical model of contact forces, the solutions and simulations based on numerical method were implemented via the use of the commercial software, **Adams**-the multibody dynamics simulation by MSC Software. In the numerical solution, the soft finger is divided into 6 segments, and each segment is the equivalent link as in the theoretical model and their configuration parameters are determined by the theoretical equations.

The length and mass of each link are presented in Table 1.

Table 1. Length and mass of the equivalent link.

Link i^{th}	1	2	3	4	5	6
Length (mm)	18	18	18	18	18	10
Mass (g)	3.94	3.94	3.94	3.94	4.05	1.36

The stiffness value k_i of the torsional spring i^{th} is determined from equation (29) with the virtual concentrated force $F = 0.25(N)$. The calculated stiffness of the torsional springs is shown in Table 2.

Table 2. Torsional stiffness values of equivalent joint.

Joint	1	2	3	4	5	6
Torsional stiffness [N.mm/degree]	4.12	1.95	1.87	1.68	1.62	1.12

After determining the values of torsional spring, the values of torsional moments T_i acting on the rotation joint i^{th} can be calculated based on equation (24), where the angle φ_j is calculated from equation (23). The values of torsional moments T_i with different pressures are shown in Table 3.

The values of the moments with different pressures in Table 3 and the torsional stiffness in Table 2 are the setting parameters in the numerical simulation model. The simulated deformation of the soft gripper via **Adams** with the equivalent discrete link model is shown in Figure 15.

Table 3. Values of the torsional moment T_i with different pressures.

P(kPa)	T_i (N.mm)					
	T_1	T_2	T_3	T_4	T_5	T_6
60	12.64	2.67	4.73	3.59	2.43	1.13
80	19.69	7.37	9.85	6.16	6.14	3.23
100	28.71	13.62	16.13	11.01	10.67	4.71
120	37.41	19.72	24.49	16.23	16.15	6.05
140	48.08	24.14	31.28	22.24	22.41	7.12
160	56.77	28.22	36.67	26.76	29.85	10.09

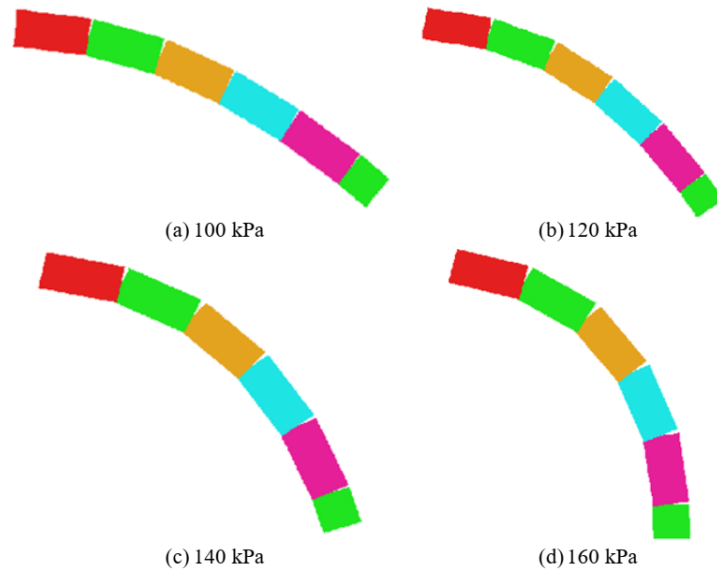


Figure 15. Simulated deformation of the soft gripper via Adams with the equivalent discrete link model

In comparison with simulated results via **Abaqus** as shown in Figure 6, it can be seen that the deformation results of the soft finger, which are obtained by the numerical solutions via the use of **Adams**, have a good agreement with its simulated results which are obtained via simulations with the use of **Abaqus**.

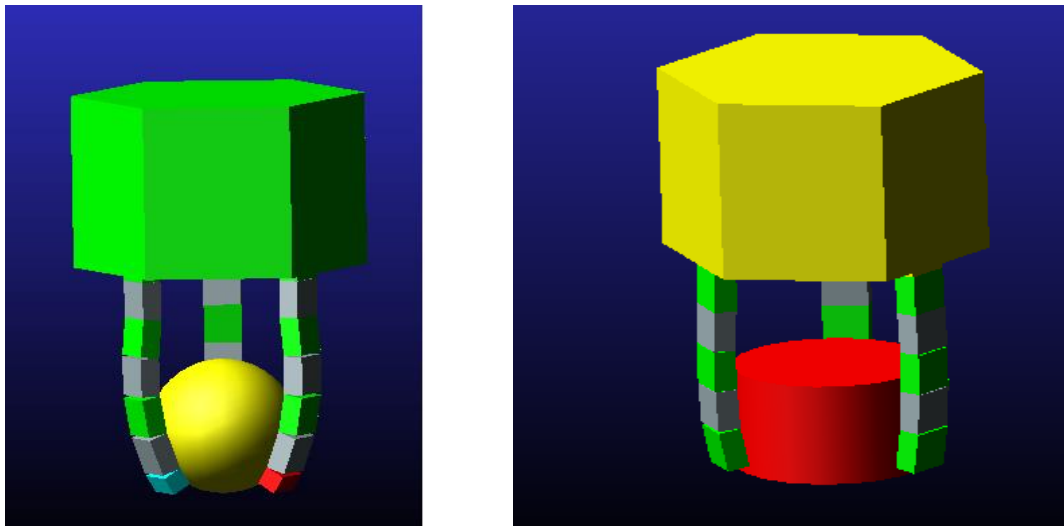


Figure 16. 3D simulations of the gripper's manipulations

Then, the numerical simulation of gripping manipulations is conducted, with the use of the proposed theoretical model of the soft finger. Figure 16 presents 3D simulations of the gripper's gripping manipulations via the use of **Adams**. The gripper has three soft

fingers and a rigid box that mimics the actual gripper. Similar to the theoretical model, the contact's configuration is set up with the following boundary conditions: (i) The adhesion force is negligible, and (ii) the contact force is calculated by using the Coulomb law with the static coefficient of 0.8 and the dynamic coefficient of 0.75. The gripping simulations are conducted with spherical and cylindrical objects. Both spherical and cylindrical objects have a diameter of 70mm and different masses. The numerical simulation is conducted with the case of the pressure value of 140kPa . The gripping simulation's process is similar to the actual gripping manipulation, including a picking step and a transferring step. Firstly, the soft gripper contacts the object at a rest position then the object is picked and moved to a higher position before it is transferred in the horizontal direction. In these steps, the speed of the gripper's motion is changed with constant acceleration; this aims to investigate the effect of dynamic motion on the capability of the soft gripper's gripping manipulations. The acceleration is set up with three values of 2m/s^2 , 5m/s^2 , and 10m/s^2 . The mass values of the object are varied, in which 150grams and 250grams are for the spherical shapes, and 80grams and 150grams are for the cylindrical shapes.

4.3. Experimental studies

The experiments were conducted to validate the effectiveness of the theoretical model, numerical simulations and investigate the real gripping capability of the soft-fingered gripper.

- Experiment on Soft finger's deformation

Firstly, the experimental measurement was conducted to validate the curvature deformation of the soft finger, which was mathematically modelled based on the theory of large beam deformation, simulated by finite element model via **Abaqus** software, and numerical solution via **Adam**. In this experimental setup, the soft finger was mounted

onto the rigid frame, and were activated by the air pressure through the pump, and the pressure's value is controlled by the air regulator. The deflection of the soft finger is estimated by using the grid board. The experimental measurement is shown in Figure 17.



Figure 17. Experimental measurement of soft finger's deformation under pressurization

- Experiment on gripping capability of gripper

Secondly, the soft gripper is connected to the robot arm, MITSUBISHI RV-12SD, which has 6-degree freedom and can move with various velocities to conduct the gripping experiments. The experimental setup is shown in Figure 18. The speed and motion trajectory of a robot arm is controlled by commercial software. The compressed air is put into the soft finger through the air tubes, and an air controller sets up its value. The contact state is assessed through the signals from strain-gauge sensors that are collected by using the LMS system. LMS is a multi-channel signal acquisition system, which can simultaneously collect signals from 16 channels with high frequency².

² <https://adtsystems.vn/en/product/lms-test-lab/> (assessed on 6/27/2022)

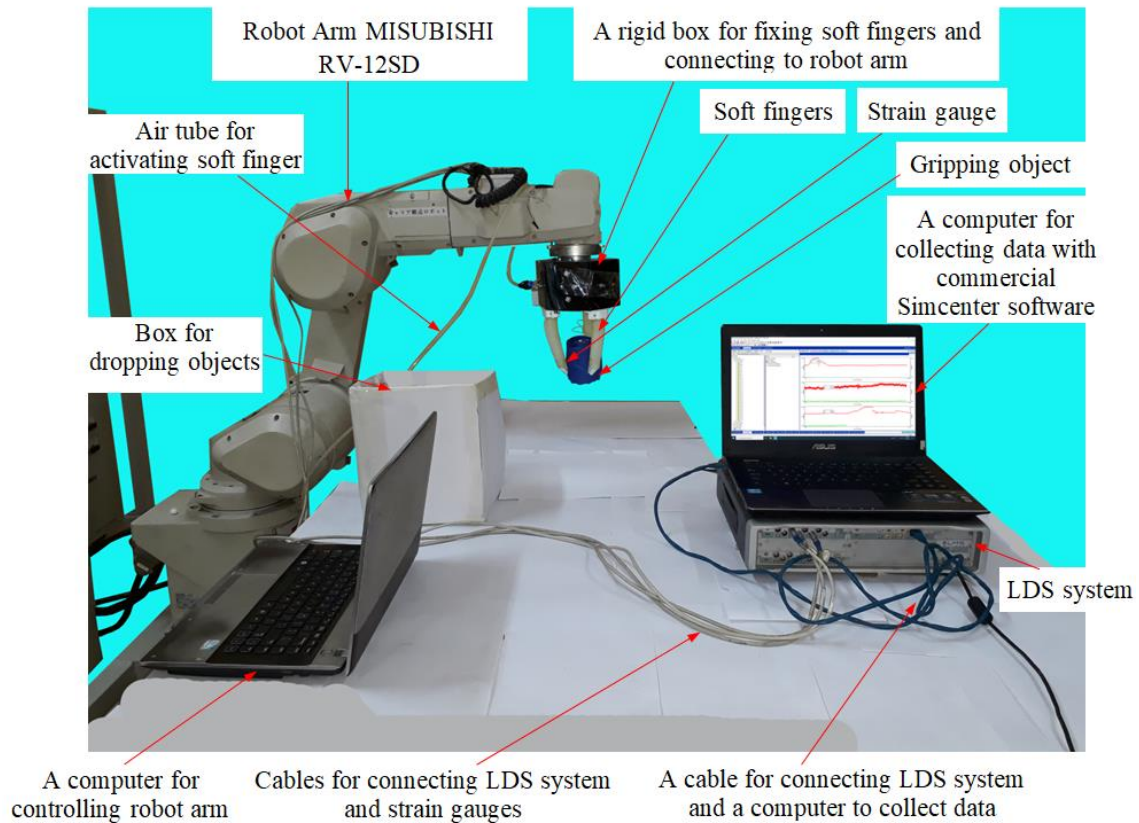


Figure 18. The experimental setup to investigate the gripping capability of the soft gripper.

The obtained data were sent to the computer through the commercial software, SIMCENTER TESTLAB, to display in real-time and save for analysis. The experiments were conducted with pick-and-place manipulation and gripping objects as used in the numerical solutions. The trajectory motions of the robot's arm were set up in horizontal and vertical directions. To precisely determine the contact point, assuming that the placement position, shape, and size of the object, including its radius and height, are predetermined. The robot arm is then controlled to position the object at the center, and the arm is moved vertically downwards to a predetermined position, allowing the soft finger to make contact at the desired contact point on the object. It is worth noting that the contact position in the experiment is setup to be identical to the contact position in the numerical simulation. This allows for accurate comparison and evaluation of the grasping capabilities of the soft finger in both experiment and numerical

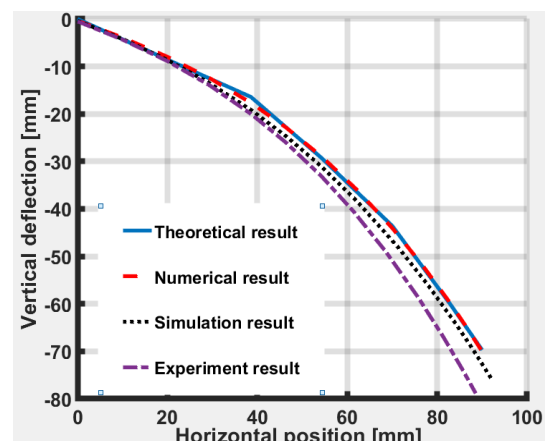
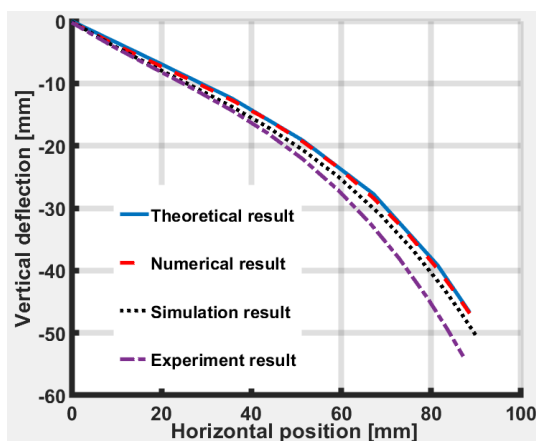
simulation. And similar to numerical simulation, the gripping is accomplished through uniform vertical contact between the inner surface of the soft finger and the gripping objects, it does not consider more complex gripping techniques such as power grasp or pinch. The object is picked and moved to the vertical-picking position, then transferred to the horizontal-placing position before the soft gripper performs the drop action. In the picking and transferring steps, the motion acceleration of the robot arm is changed, similar to the simulation setup. The gripping capability of the soft finger and object is represented by the falling phenomenon of the object, which is detected through the sudden decrease of the strain gauge's signal. The obtained signal from the strain gauge through the LMS system is the deformation amplitude at the integrated position of the strain gauge on the soft finger. By monitoring the variation of the obtained signal, the grasping capability of the soft gripper under the dynamic motion of the robot arm can be evaluated.

4.4. Results and Discussion

- Soft finger's deformation

The analysis of the curvature deformation of the soft finger was conducted using pressure values ranging from $10kPa$ to $16kPa$, which are effective in producing suitable curvature deformation. To assess the deformation of the soft finger, the vertical deflection y was measured at various horizontal positions x . Theoretical results were obtained by solving equation (16) using the integration function in MATLAB, as detailed in section 3.2. Simulation results were obtained by analyzing the displacement of nodes in the deformation simulation of soft fingers using Abaqus software, as described in section 3.1. Numerical solution results were evaluated by examining the displacement of the equivalent link simulated through Adam software, presented in section 4.2. The theoretical, simulation, and numerical solution results were then compared with experimental results obtained using the experimental setup detailed in section 4.3.

The comparison between the results is presented in Figure 19 and Figure 20. It can be observed that the numerical and theoretical results have an error of less than 5%. This is because the parameters of the equivalent rigid links in the numerical solution model via the Adam software, are determined from the theoretical equations. In the theoretical model, the material is assumed to be linear, and the non-linearity property is neglected, whereas the simulation takes into account the physical nonlinearity of the soft materials using the coefficients of the Yeoh model for non-linear material. Which is why the numerical and theoretical results are lower than the simulation results. The experimental results are also higher than the theoretical, numerical, and simulation results. However, the maximum error between the theoretical and experimental results is less than 13%, which confirms the effectiveness of the proposed theoretical model. The small error in the calculated result also indicates that the non-linearity of large deformations has a greater impact on the deformation of the soft finger than the physical non-linearity of the soft material. Thus, the proposed cantilever beam model can serve as an explicit mathematical model for the curvature shape of a soft finger. The good agreement between the numerical solution and theoretical results demonstrates the accuracy of modelling soft fingers using the equivalent rigid links model, enabling the development of a dynamic gripping model and investigation of the gripping capability of the soft-fingered gripper.



(a) 100 kPa

(b) 120 kPa

Figure 19. Finger's deformation under different pressurization 100 kPa, 120 kPa

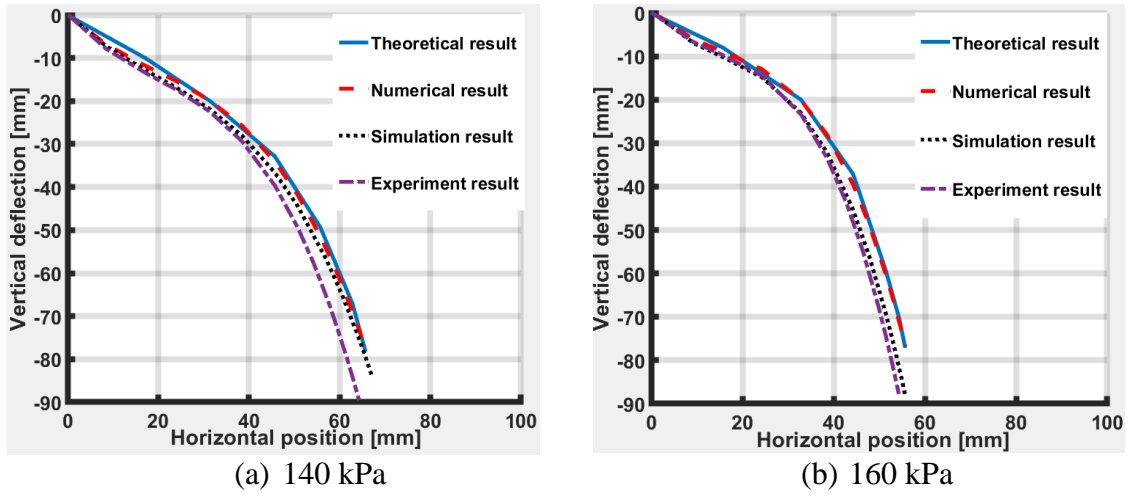


Figure 20. Finger's deformation under different pressurization 140 kPa, 160 kPa

- Gripping capability of the gripper

In terms of the grasping capability of the gripper, the simulation results are presented in Figure 21 to Figure 24. Where the grasping state of the soft finger can be evaluated through the change of displacements of the gripping objects. In the picking step, the displacement is increased to the constant value then its value has remained in the transferring step. In these steps, the fall of the grasping objects is represented by a sudden decrease in the value of displacement.

Figure 21 shows that the gripper can complete the grasping manipulation with the spherical object's masses of 150grams and the acceleration of $2m/s^2$, $5m/s^2$, but with the higher acceleration of $10m/s^2$ the grasping manipulation is failed in the transferring step. In Figure 22, when the object's mass is increased to 250grams, the falling phenomenon occurs with all conditions of the accelerations. The object falls immediately in the picking step for accelerations of $5m/s^2$ and $10m/s^2$. In Figure 23 and Figure 24, it can be seen that the ability of the grasping manipulation with cylindrical objects is similar to that of spherical objects. Nonetheless, the gripper can complete the gripping manipulation with a smaller mass for the case of the cylindrical object, in comparison

with the spherical object. Figure 24 also points out that the gripper cannot pick the cylindrical object with masses of 150grams and the acceleration of $10m/s^2$.

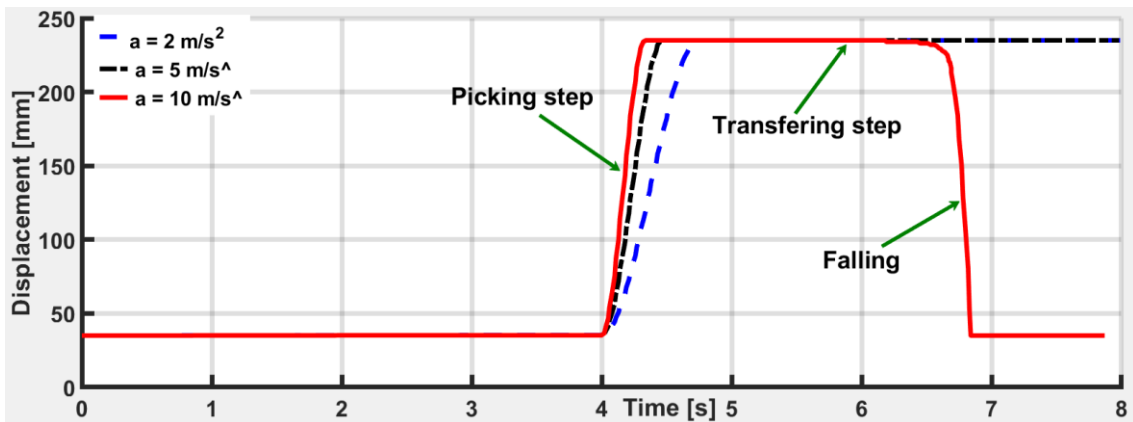


Figure 21. The displacement of the spherical object of 150grams with different accelerations.

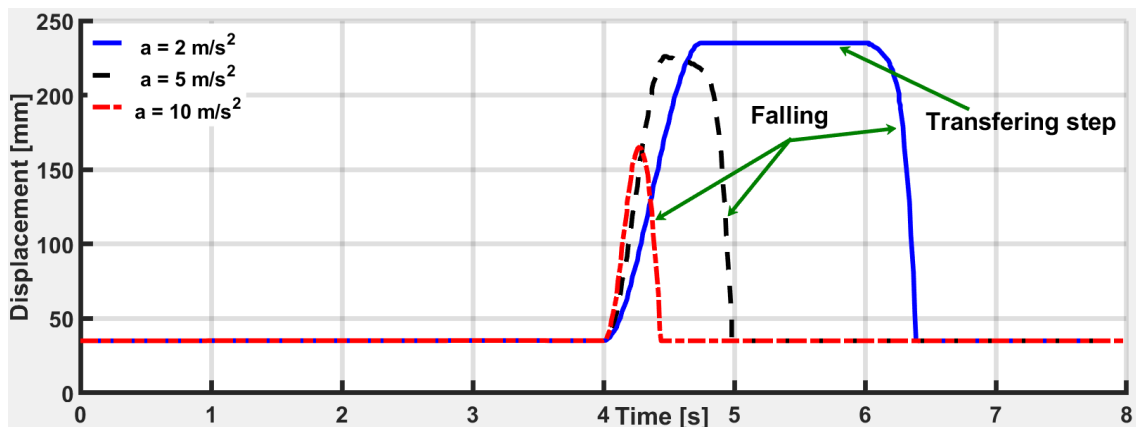


Figure 22. The displacement of the spherical object of 250grams with different accelerations.

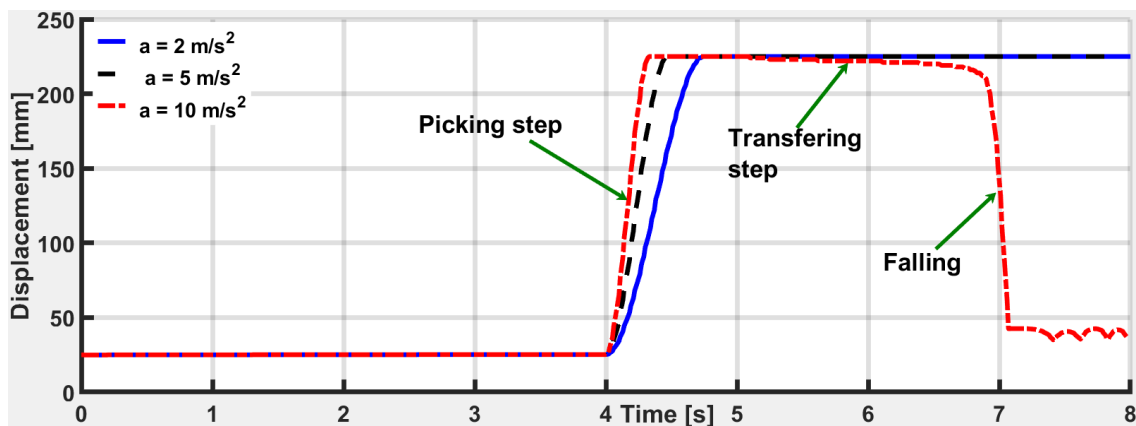


Figure 23. The displacement of the cylindrical object of 80grams with different accelerations.

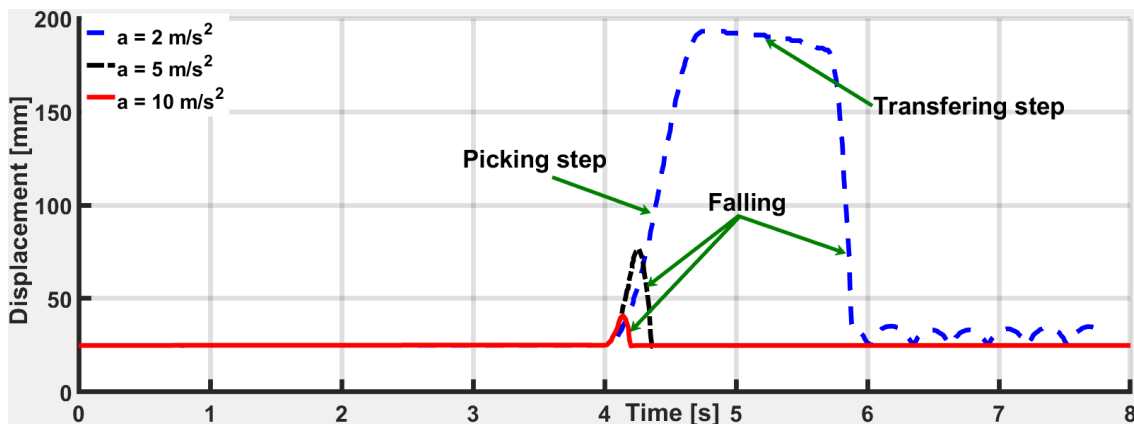


Figure 24. The displacement of the cylindrical object of 150grams with different accelerations.

The gripping capability of the gripper is then validated and analysed by experiments. The experimental results are presented in Figure 25 to Figure 28. From the experimental results, it can be seen that, during the gripping manipulation, the obtained signal of the strain gauge can be divided into four main stages as follows. In the first stage, the gripper moves from the original position to contact with the object. During this stage, the soft finger is not deformed, thus the strain amplitude of the strain gauge is approximately 0. In the second stage, the gripper is deformed under the activation of compressed air to generate the curvature shape. When the air pressure is activated, the gripper begins to contact the object and performs the gripping operation, leading to the increased deformation of the soft fingers. In this process, the strain magnitude increases linearly until the gripper finishes lifting the object from the original position to the lifting position. In the next stage, the gripper carries out the object in the horizontal direction, the strain gauge signals reflect the contact behaviour between the soft finger and gripping object, it can be stable or unstable, depending on the shape and the mass of the gripping object, and the acceleration of the gripper's motion. In the final stage, the gripper performs the dropping

step and returns to the free state, the strain magnitude bounces back to the value of 0. In the grasping manipulation of the gripper, the falling phenomenon of the object can be detected by the sudden decrease to the zero value of the strain magnitude, which is similar to the precipitous decrease of the displacement values in numerical simulation.

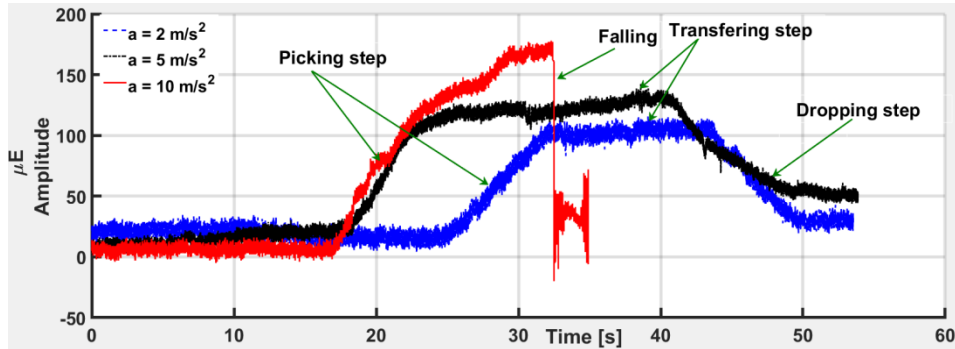


Figure 25. Strain amplitude in the case of grasping manipulation with spherical object's masses of 150grams and different acceleration motion of robot arm.

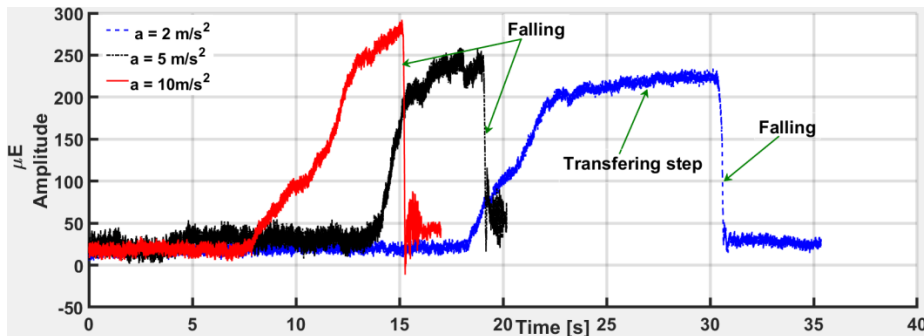


Figure 26. Strain amplitude in the case of grasping manipulation with spherical object's masses of 250 grams and different acceleration motion of robot arm.

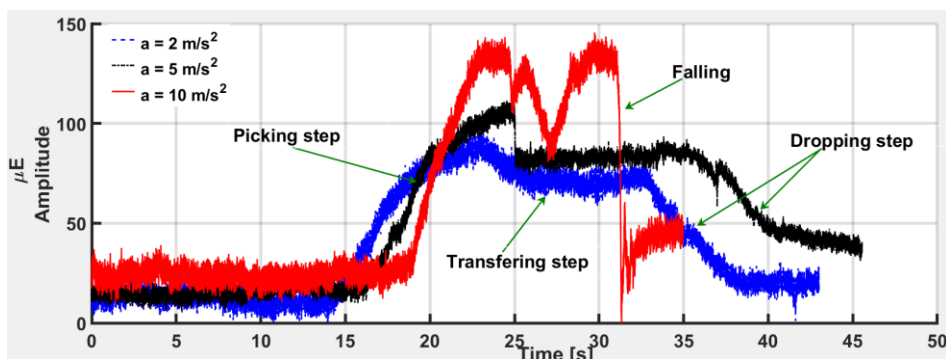


Figure 27. Strain amplitude in the case of grasping manipulation with cylindrical object's masses of 80grams and different acceleration motion of robot arm.

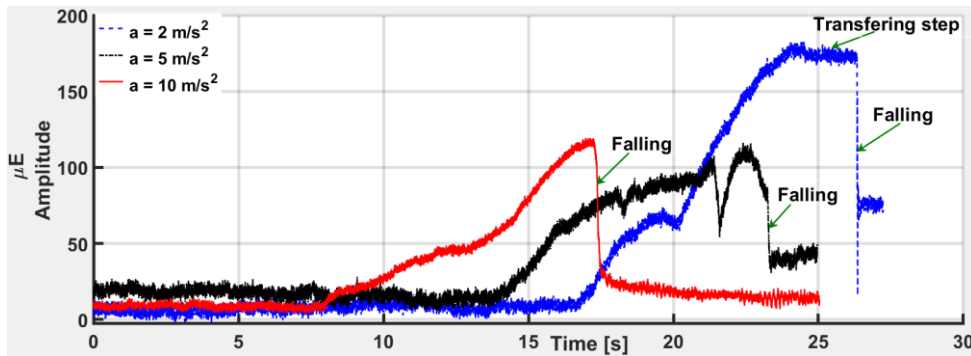


Figure 28. Strain amplitude in the case of grasping manipulation with cylindrical object's masses of 150grams and different acceleration motion of robot arm.

The results presented in Figure 25 show that, in the case of the spherical object with a mass of 150grams, the gripper can complete the pick-place manipulation with the acceleration of $2m/s^2$ and $5m/s^2$, the process of picking, transferring and dropping objects has been successfully performed but the falling phenomenon occurs with the gripping acceleration of $10m/s^2$ which is represented by a sudden decrease of the strain magnitude. That is similar to the simulation results shown in Figure 21. Similar to Figure 22, the experimental results in Figure 26 also validate the incomplete gripping manipulation with the spherical object's mass of 250grams, the falling phenomenon occurs under all values of the accelerations and with higher values of the acceleration of $5m/s^2$ and $10m/s^2$ the object is fallen even in the picking step.

The numerical solution with the cylindrical objects is validated by experimental results shown in Figure 27 and Figure 28. The experimental results also point out that the instability grasping performance of the soft gripper with cylindrical objects is more strongly than that of spherical objects. Therefore, it can be concluded that the grasping ability with spherical objects is better than the one with cylindrical objects. And the possible mass of the spherical objects is significantly greater than that of the cylindrical objects. It is similar to the numerical solution results and it can be explained as follows. Due to the curved deformation of the soft finger, the contact area of the soft finger is

much better with a spherical object than with a cylindrical object. The acknowledgment of numerical simulation and experimental results confirm that beyond the mass and of grasping objects, the acceleration of the robot arm's motion is also an important factor when evaluating the gripping capability and performance of the soft gripper. This factor must be taken into account in the design, fabrication, and analysis of the soft gripper.

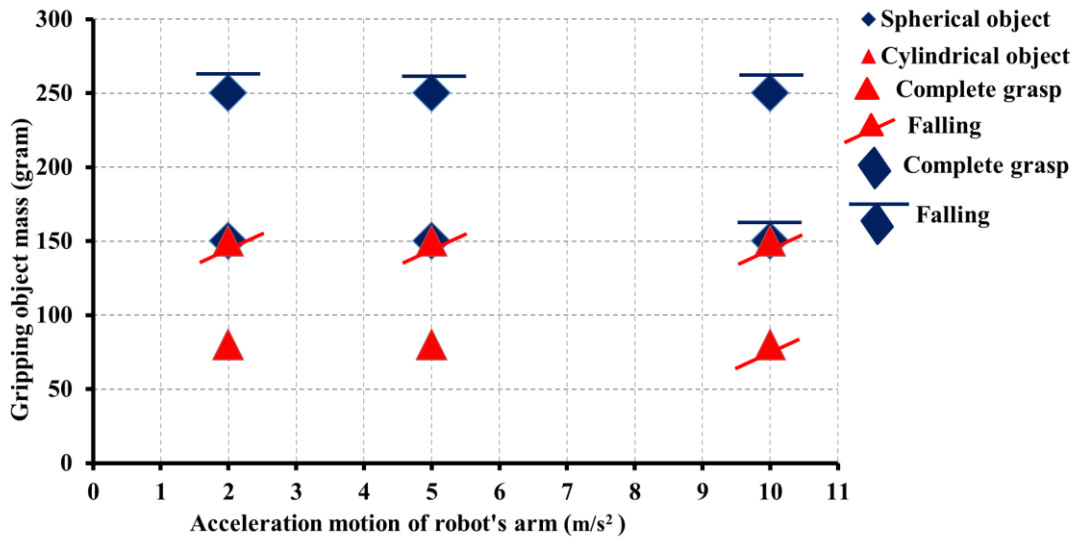


Figure 29. Summary result of gripping capability of soft gripper, confirm by experiment and numerical simulations.

More importantly, the experimental results confirm the effectiveness of the numerical solutions based on the proposed theoretical models, especially when investigating the capability and performance of soft grippers. From the similarity between the theoretical approach and experiments, the gripping capability of the soft gripper is summarised in Figure 29.

5. Summary and conclusions

Soft grippers offer several advantages over traditional rigid grippers, such as safe interaction with fragile objects and operating in unpredictable environments. However, the design of soft grippers that are both easy to fabricate and model while maintaining their gripping ability remains an open research issue that requires further investigation.

Additionally, the working ability and stability of soft grippers during gripping processes under dynamic motions of robot arm have not been thoroughly studied yet. Therefore, more in-depth studies are needed to address these design and operational challenges for soft grippers. This is more and more important and necessary when considering the emerging trends of using collaborative robots in Smart Manufacturing and Industry 4.0.

This study introduces an innovative soft robotic gripper that effectively performs grasping tasks based on the deformation of its soft fingers. The soft finger is designed based on the mechanism of an asymmetric soft actuator with a variable cross-section, which has a simple design. The gripper is fabricated using a molding method for the soft finger and 3D printing and CNC cutting machines for the other components. Three strain-gauge sensors are embedded in the soft fingers to detect the contact manner during grasping manipulation. The soft finger's deformation is then described by the explicit mathematical model based on the Euler–Bernoulli theory of large deformation beam. Next, by proposing an equivalent model with joint and link designs, the dynamics of the soft gripper can be mathematically modeled and simulated. The novel mathematical modeling and numerical solutions were successfully developed and experimentally validated to analyze the effects of dynamic motions on the gripper's grasping capability. The experiment measures the variation of the strain gauge's magnitude to assess the contact manner between the soft finger and the grasping object. The similarity of numerical and experimental results demonstrates that the soft gripper's grasping capability depends on the mass of the grasped objects and the acceleration motion's value. This similarity also confirms that the proposed method to investigate the grasping capability of the soft gripper is valid.

In addition, the theoretical approach used in this study based on the large beam deformation model has the potential to be extended for modeling the curvature shape of

other soft actuators. Additionally, the method of assigning the soft finger by the equivalent model with joints, links, and numerical solutions can also be applied to analyze the dynamic gripping manipulation and gripping capability of other soft grippers with specific structures as in the studies (Li et al. 2022; Qi et al. 2022; Zang et al. 2020). That has important implications in the design, fabrication, and evaluation of the working ability of soft grippers. For this purpose, the equivalence models can be varied with different moments at different positions and non-uniform joint stiffness (Sinatra et al. 2019; Zheng et al. 2020). More complex mathematical models are required to determine these parameters based on our proposed method.

Note that to validate the theoretical dynamics models, it is necessary to verify certain parameters while the gripper-gripping object system is in motion. However, measuring the acceleration of the fingers and assessing the contact force between the object and the fingers becomes exceedingly challenging when the gripping system is undergoing acceleration, primarily due to the complications associated with mounting the measuring device. Experimental study on the contact forces between the soft fingers and the object, and other dynamic effects of the fingers-object system will be the future work of this investigation.

Appendix

$$Y_C = \frac{-e\pi r_i^2 - \frac{2}{3} \frac{R \sin \alpha \cos^2 \alpha - r_i \sin \alpha}{(\alpha - \sin \alpha \cos \alpha)} R^2 (\alpha - \sin \alpha \cos \alpha)}{\pi(R^2 - r_i^2) - R^2 (\alpha - \sin \alpha \cos \alpha)} \quad (43)$$

$$Y_{C3} = -\frac{2}{3} \frac{R \sin \alpha}{\alpha} \quad (44)$$

$$Y_{C5} = \frac{-2}{3} R \cos \alpha \quad (45)$$

Replacing Y_C , Y_{C3} , Y_{C5} in equations (43), (44), (45) into equations (39), (40), (41), (42), then replacing I_{xC1} , I_{xC2} and I_{xC4} into equation (38), the value of inertial moment I_{xC} is determined.

Funding

This work was supported by the Vingroup Innovation Foundation (VINIF) annual research support program under Grant VINIF.2019.DA08.

References

- ACAR, Osman, Hacı SAĞLAM, and Ziya ŞAKA. 2021. "Evaluation of Grasp Capability of a Gripper Driven by Optimal Spherical Mechanism." *Mechanism and Machine Theory* 166. doi: 10.1016/j.mechmachtheory.2021.104486.
- Al-Rubai, Mohammed, Thassyo Pinto, Chunqi Qian, and Xiaobo Tan. 2019. "Soft Actuators with Stiffness and Shape Modulation Using 3D-Printed Conductive Polylactic Acid Material." *Soft Robotics* 6(3). doi: 10.1089/soro.2018.0056.
- Anon. 2006. *Nonlinear Structural Engineering*.
- Bhattacharya, Srijan, Bikash Bepari, and Subhasis Bhaumik. 2014. "IPMC-Actuated Compliant Mechanism-Based Multifunctional Multifinger Microgripper." Pp. 312–25 in *Mechanics Based Design of Structures and Machines*. Vol. 42. Taylor and Francis Inc.
- Bullock, Ian M., Raymond R. Ma, and Aaron M. Dollar. 2013. "A Hand-Centric Classification of Human and Robot Dexterous Manipulation." *IEEE Transactions on Haptics* 6(2). doi:

10.1109/TOH.2012.53.

- Burstedt, Magnus K. O., J. Randall Flanagan, and Roland S. Johansson. 1999. "Control of Grasp Stability in Humans under Different Frictional Conditions during Multidigit Manipulation." *Journal of Neurophysiology* 82(5). doi: 10.1152/jn.1999.82.5.2393.
- Carpi, Federico, Claudio Salaris, and Danilo De Rossi. 2007. "Folded Dielectric Elastomer Actuators." *Smart Materials and Structures* 16(2). doi: 10.1088/0964-1726/16/2/S15.
- Chase, Robert P., Robert H. Todd, Larry L. Howell, and Spencer P. Magleby. 2011. "A 3-D Chain Algorithm with Pseudo-Rigid-Body Model Elements." *Mechanics Based Design of Structures and Machines* 39(1). doi: 10.1080/15397734.2011.541783.
- Chu, A. M., C. D. Nguyen, X. B. Duong, A. V. Nguyen, T. A. Nguyen, C. H. Le, and Michael Packianather. 2022. "A Novel Mathematical Approach for Finite Element Formulation of Flexible Robot Dynamics." *Mechanics Based Design of Structures and Machines* 50(11). doi: 10.1080/15397734.2020.1820874.
- Dang, Hoang Minh, Chi Thanh Vo, Viet Duc Nguyen, Hai Nam Nguyen, Anh Vang Tran, and Van Binh Phung. 2021. "A Method for Determining Parameters of Hyperelastic Materials and Its Application in Simulation of Pneumatic Soft Actuator." *International Journal of Computational Materials Science and Engineering* 10(3). doi: 10.1142/S2047684121500172.
- Galloway, Kevin C., Kaitlyn P. Becker, Brennan Phillips, Jordan Kirby, Stephen Licht, Dan Tchernov, Robert J. Wood, and David F. Gruber. 2016. "Soft Robotic Grippers for Biological Sampling on Deep Reefs." *Soft Robotics* 3(1). doi: 10.1089/soro.2015.0019.
- Guo, J., K. Elgeneidy, C. Xiang, N. Lohse, L. Justham, and J. Rossiter. 2018. "Soft Pneumatic Grippers Embedded with Stretchable Electroadhesion." *Smart Materials and Structures* 27(5). doi: 10.1088/1361-665X/aab579.
- Haibin, Yin, Kong Cheng, Li Junfeng, and Yang Guilin. 2018. "Modeling of Grasping Force for a Soft Robotic Gripper with Variable Stiffness." *Mechanism and Machine Theory* 128. doi: 10.1016/j.mechmachtheory.2018.05.005.
- Hasan, Waris, Lucas Gerez, and Minas Liarokapis. 2020. "Model-Free, Vision-Based Object

- Identification and Contact Force Estimation with a Hyper-Adaptive Robotic Gripper.” Pp. 9514–20 in *IEEE International Conference on Intelligent Robots and Systems*. Institute of Electrical and Electronics Engineers Inc.
- Ho, Van, and Shinichi Hirai. 2017. “Design and Analysis of a Soft-Fingered Hand With Contact Feedback.” *IEEE Robotics and Automation Letters* 2(2). doi: 10.1109/LRA.2016.2645120.
- Howard, W. Stamps, and Vijay Kumar. 1996. “On the Stability of Grasped Objects.” *IEEE Transactions on Robotics and Automation* 12(6). doi: 10.1109/70.544773.
- Hu, Qiqiang, Erbao Dong, and Dong Sun. 2021. “Soft Gripper Design Based on the Integration of Flat Dry Adhesive, Soft Actuator, and Microspine.” *IEEE Transactions on Robotics* 37(4). doi: 10.1109/TRO.2020.3043981.
- Hubbard, Amber M., Russell W. Mailen, Mohammed A. Zikry, Michael D. Dickey, and Jan Genzer. 2017. “Controllable Curvature from Planar Polymer Sheets in Response to Light.” *Soft Matter* 13(12). doi: 10.1039/c7sm00088j.
- Hussain, Irfan, Monica Malvezzi, Dongming Gan, Zubair Iqbal, Lakmal Seneviratne, Domenico Prattichizzo, and Federico Renda. 2021. “Compliant Gripper Design, Prototyping, and Modeling Using Screw Theory Formulation.” *International Journal of Robotics Research* 40(1). doi: 10.1177/0278364920947818.
- Kleeberger, Kilian, Richard Bormann, Werner Kraus, and Marco F. Huber. 2020. “A Survey on Learning-Based Robotic Grasping.” *Current Robotics Reports* 1(4):239–49. doi: 10.1007/s43154-020-00021-6.
- Le, Chi Hieu, Dang Thang Le, Daniel Arey, Popan Gheorghe, A. M. Chu, X. B. Duong, T. T. Nguyen, T. T. Truong, Chander Prakash, Shi Tian Zhao, Jamaluddin Mahmud, James Gao, and M. S. Packianather. 2020. “Challenges and Conceptual Framework to Develop Heavy-Load Manipulators for Smart Factories.” *International Journal of Mechatronics and Applied Mechanics* 2(8). doi: 10.17683/ijomam/issue8.58.
- Lee, Chiwon, Myungjoon Kim, Yoon Jae Kim, Nhayoung Hong, Seungwan Ryu, H. Jin Kim, and Sungwan Kim. 2017. “Soft Robot Review.” *International Journal of Control, Automation and Systems* 15(1).

- Li, Shuguang, Samer A. Awale, Katharine E. Bacher, Thomas J. Buchner, Cosimo Della Santina, Robert J. Wood, and Daniela Rus. 2022. "Scaling Up Soft Robotics: A Meter-Scale, Modular, and Reconfigurable Soft Robotic System." *Soft Robotics* 9(2). doi: 10.1089/soro.2020.0123.
- Liu, S., M. Van, Z. Chen, J. Angeles, and C. Chen. 2021. "A Novel Prosthetic Finger Design with High Load-Carrying Capacity." *Mechanism and Machine Theory* 156. doi: 10.1016/j.mechmachtheory.2020.104121.
- Llop-Harillo, Immaculada, Antonio Pérez-González, Julia Starke, and Tamim Asfour. 2019. "The Anthropomorphic Hand Assessment Protocol (AHAP)." *Robotics and Autonomous Systems* 121. doi: 10.1016/j.robot.2019.103259.
- Loeve, Arjo J., Oscar S. Van De Ven, Johan G. Vogel, Paul Breedveld, and Jenny Dankelman. 2010. "Vacuum Packed Particles as Flexible Endoscope Guides with Controllable Rigidity." *Granular Matter* 12(6):543–54. doi: 10.1007/s10035-010-0193-8.
- Manti, Mariangela, Vito Cacucciolo, and Matteo Cianchetti. 2016. "Stiffening in Soft Robotics: A Review of the State of the Art." *IEEE Robotics and Automation Magazine* 23(3):93–106. doi: 10.1109/MRA.2016.2582718.
- Marette, Alexis, Alexandre Poulin, Nadine Besse, Samuel Rosset, Danick Briand, and Herbert Shea. 2017. "Flexible Zinc–Tin Oxide Thin Film Transistors Operating at 1 KV for Integrated Switching of Dielectric Elastomer Actuators Arrays." *Advanced Materials* 29(30). doi: 10.1002/adma.201700880.
- Mata Amritanandamayi Devi, Ganesha Udupa, and Pramod Sreedharan. 2018. "A Novel Underactuated Multi-Fingered Soft Robotic Hand for Prosthetic Application." *Robotics and Autonomous Systems* 100. doi: 10.1016/j.robot.2017.11.005.
- My, Chu A., and Duong X. Bien. 2020. "New Development of the Dynamic Modeling and the Inverse Dynamic Analysis for Flexible Robot." *International Journal of Advanced Robotic Systems* 17(4). doi: 10.1177/1729881420943341.
- Park, Tongil, Keehoon Kim, Sang Rok Oh, and Youngsu Cha. 2020. "Electrohydraulic Actuator for a Soft Gripper." *Soft Robotics* 7(1). doi: 10.1089/soro.2019.0009.

- Qi, Qiukai, Chaoqun Xiang, Van Anh Ho, and Jonathan Rossiter. 2022. "A Sea-Anemone-Inspired, Multifunctional, Bistable Gripper." *Soft Robotics* 9(6). doi: 10.1089/soro.2020.0176.
- Ren, Tao, Yingtian Li, Menghong Xu, Yunquan Li, Caihua Xiong, and Yonghua Chen. 2020. "A Novel Tendon-Driven Soft Actuator with Self-Pumping Property." *Soft Robotics* 7(2). doi: 10.1089/soro.2019.0008.
- Roa, Máximo A., and Raúl Suárez. 2015. "Grasp Quality Measures: Review and Performance." *Autonomous Robots* 38(1). doi: 10.1007/s10514-014-9402-3.
- Rodrigue, Hugo, Wei Wang, Dong Ryul Kim, and Sung Hoon Ahn. 2017. "Curved Shape Memory Alloy-Based Soft Actuators and Application to Soft Gripper." *Composite Structures* 176. doi: 10.1016/j.compstruct.2017.05.056.
- Shintake, Jun, Samuel Rosset, Bryan Schubert, Dario Floreano, and Herbert Shea. 2016. "Versatile Soft Grippers with Intrinsic Electroadhesion Based on Multifunctional Polymer Actuators." *Advanced Materials* 28(2). doi: 10.1002/adma.201504264.
- Sinatra, Nina R., Clark B. Teeple, Daniel M. Vogt, Kevin Kit Parker, David F. Gruber, and Robert J. Wood. 2019. "Ultragentle Manipulation of Delicate Structures Using a Soft Robotic Gripper." *Science Robotics* 4(33). doi: 10.1126/SCIROBOTICS.AAX5425.
- Spiers, Adam J., Minas V. Liarokapis, Berk Calli, and Aaron M. Dollar. 2016. "Single-Grasp Object Classification and Feature Extraction with Simple Robot Hands and Tactile Sensors." *IEEE Transactions on Haptics* 9(2). doi: 10.1109/TOH.2016.2521378.
- Stuart, Hannah, Shiquan Wang, Oussama Khatib, and Mark R. Cutkosky. 2017. "The Ocean One Hands: An Adaptive Design for Robust Marine Manipulation." *International Journal of Robotics Research* 36(2). doi: 10.1177/0278364917694723.
- Terrile, Silvia, Miguel Argüelles, and Antonio Barrientos. 2021. "Comparison of Different Technologies for Soft Robotics Grippers." *Sensors* 21(9).
- Vedhagiri, Godwin Ponraj Joseph, Avataram Venkatavaradan Prituja, Changsheng Li, Guoniu Zhu, Nitish V. Thakor, and Hongliang Ren. 2019. "Pinch Grasp and Suction for Delicate Object Manipulations Using Modular Anthropomorphic Robotic Gripper with Soft Layer

- Enhancements.” *Robotics* 8(3). doi: 10.3390/robotics8030067.
- Wang, Daoming, Yan Xiong, Bin Zi, Sen Qian, Zhengyu Wang, and Weidong Zhu. 2021. “Design, Analysis and Experiment of a Passively Adaptive Underactuated Robotic Hand with Linkage-Slider and Rack-Pinion Mechanisms.” *Mechanism and Machine Theory* 155. doi: 10.1016/j.mechmachtheory.2020.104092.
- Wang, Michael Yu, and Shikui Chen. 2009. “Compliant Mechanism Optimization: Analysis and Design with Intrinsic Characteristic Stiffness.” *Mechanics Based Design of Structures and Machines* 37(2). doi: 10.1080/15397730902761932.
- Wang, Wei, and Sung Hoon Ahn. 2017. “Shape Memory Alloy-Based Soft Gripper with Variable Stiffness for Compliant and Effective Grasping.” *Soft Robotics* 4(4). doi: 10.1089/soro.2016.0081.
- Wang, Zhongkui, and Shinichi Hirai. 2017. “Soft Gripper Dynamics Using a Line-Segment Model With an Optimization-Based Parameter Identification Method.” *IEEE Robotics and Automation Letters* 2(2). doi: 10.1109/LRA.2017.2650149.
- Watanabe, Tetsuyou, Kota Morino, Yoshitatsu Asama, Seiji Nishitani, and Ryo Toshima. 2021. “Variable-Grasping-Mode Gripper with Different Finger Structures for Grasping Small-Sized Items.” *IEEE Robotics and Automation Letters* 6(3):5673–80. doi: 10.1109/LRA.2021.3083243.
- Webster, Robert J., and Bryan A. Jones. 2010. “Design and Kinematic Modeling of Constant Curvature Continuum Robots: A Review.” *International Journal of Robotics Research* 29(13). doi: 10.1177/0278364910368147.
- Wen, Ruoshi, Kai Yuan, Qiang Wang, Shuai Heng, and Zhibin Li. 2020. “Force-Guided High-Precision Grasping Control of Fragile and Deformable Objects Using SEMG-Based Force Prediction.”
- Yap, Hong Kai, Hui Yong Ng, and Chen Hua Yeow. 2016. “High-Force Soft Printable Pneumatics for Soft Robotic Applications.” *Soft Robotics* 3(3). doi: 10.1089/soro.2016.0030.
- Yarali, Ebrahim, Reza Noroozi, Ali Moallemi, Ali Taheri, and Mostafa Baghani. 2020.

“Developing an Analytical Solution for a Thermally Tunable Soft Actuator under Finite Bending.” *Mechanics Based Design of Structures and Machines*. doi: 10.1080/15397734.2020.1763182.

Zang, Hongbin, Bing Liao, Xin Lang, Zi Long Zhao, Weifeng Yuan, and Xi Qiao Feng. 2020. “Bionic Torus as a Self-Adaptive Soft Grasper in Robots.” *Applied Physics Letters* 116(2). doi: 10.1063/1.5128474.

Zheng, Xingwen, Ningzhe Hou, Pascal Johannes Daniel Dinjens, Ruifeng Wang, Chengyang Dong, and Guangming Xie. 2020. “A Thermoplastic Elastomer Belt Based Robotic Gripper.” in *IEEE International Conference on Intelligent Robots and Systems*.

Zhong, Guoliang, Yangdong Hou, and Weiqiang Dou. 2019. “A Soft Pneumatic Dexterous Gripper with Convertible Grasping Modes.” *International Journal of Mechanical Sciences* 153–154. doi: 10.1016/j.ijmecsci.2019.02.028.